Iconography of Icosahedra. Calculations of Metallic Energies and Relative Stabilities of Stereoisomers of Binary Icosahedral Clusters

Boon K. Teo,* Alex Strizhev, Ron Elber, and Hong Zhang*

Department of Chemistry, University of Illinois at Chicago, 845 W. Taylor Street, Rm. 4500, Chicago, Illinois 60607

Received March 3, 1997

The first part of this paper provides a complete iconography of all possible stereoisomers of a binary icosahedron (a total of 96 for a noncentered A_nB_{12-n} ($n = 0-12$) and 192 for a centered A_nB_{13-n} ($n = 0-13$) icosahedron) by utilizing a simple symmetry-based algorithm. The second part of this paper deals with the relative stabilities of these stereoisomers for a given combination of A and B atoms. A simple theory, based on the Lennard-Jones potential and cohesive energies of transition metals, has been developed in order to model metallic bonding in a metal cluster. This provides a relative measure of the strengths of metal−metal bonds in a mixed-metal cluster and hence the relative energetic stabilities of various stereoisomers. The utility of this simple theory is illustrated by applying it to all possible stereoisomers of binary icosahedral clusters A_nB_{13-n} ($n = 0-13$) containing the Au−Ag, Au−Ni, and Au−Pt combinations. Considerable insight into metal−metal interactions in mixed-metal systems can be gained by detailed analysis of the contributions—covalent vs ionic—to the metallic bonding energy. Indeed, on the basis of the calculated energies, two simple rules—the Strong-Bond rule and the Hetero-Bond rule—were formulated. These rules are useful in predicting the relative stabilities of these stereoisomers, thereby furthering the understanding of site preference in multimetallic systems, including mixed-metal clusters, metal alloy systems, multimetallic catalysts, etc.

I. Introduction

The past decade has seen an unusual surge of experimental and theoretical activities in cluster chemistry involving the icosahedron.[1−11] Recent developments in metal cluster chemistry, in particular, have resulted in a variety of metal clusters whose structures are based on an icosahedron.[5−11] The tendency of clusters to form the icosahedral structure may be termed "icosahedricity".[11m] An icosahedron can also serve as the basic building block for high-nuclearity metal clusters; for example, our recent work in this area gave rise to a series of bi- or trimetallic supraclusters whose metal framework can be described as vertex-sharing polyicosahedra[11] in which the 13-atom centered icosahedra are fused together via sharing of vertex

(1) An icosahedron has twelve vertices, twenty trangular faces, and thirty edges. The icosahedral I_h symmetry is the highest possible point group symmetry in three dimensions (except for the spherical harmonics point group, K_h).

(2) (a) Lipscomb, W. N. *Boron Hydrides* W. A. Benjamin, Inc.: New York, (**1963**). (b) Lipscomb, W. N.; Wunderlich, J. A *J. Am. Chem. Soc.* **1960**, *82*, 4427. (c) Muetterties, E. L.; Merrifield, R. E.; Miller, H. C.; Knoth, W. H.; Downing, J. R. *J. Am. Chem. Soc.* **1962**, *84*, 2506.

(3) (a) Zheng, Z.; Knobler, C. B.; Mortimer, M. D.; Kong, G.; Hawthorne, M. F. *Inorg. Chem.* **1996**, *35*, 1235−1243. (b) Yang, X. G.; Knobler, C. B.; Zheng, Z. P.; Hawthorne, M. F. *J. Am. Chem. Soc.* **1994**, *116*, 7142. (c) Harwell, D. E.; Mortimer, M. D.; Knobler, C. B.; Anet F. A. L.; Hawthorne, M. F. *J. Am. Chem. Soc.*, **1996**, *118*, 2679.

(4) (a) Grimes, R. N. *Carboranes*, Academic: New York, 1970. (b) Grimes, R. N. *Coord. Chem. Rev.* **1995**, *143*, 71. (c) Beall, H. In *Boron Hydride Chemistry*; Muetterties, E. L., Ed.; Academic: New York, 1975; p 301. (d) Shore, S. G. *Pure Appl. Chem.* **1994**, *66*, 263. (e) Knoth, W. H. *Inorg. Chem.* **1971**, *10*, 598.

(5) (a) Dong, Z. C.; Corbett, J. D. *J. Am. Chem. Soc.* **1995**, *117*, 6447. (b) Carr, N.; Mullica, D. F.; Sappenfield, E. L.; Stone, F. G. A. *Inorg. Chem.* **1994**, *33*, 1666−1673. (c) Kester, J. G.; Keller, D.; Huffman, J. C.; Benefiel, M. A.; Geiger, W. E., Jr.; Atwood, C.; Siedle, A. R.; Korba, G. A.; Todd, L. J. *Inorg. Chem.* **1994**, *33*, 5438.

(6) Pignolet, L. H.; Aubart, M. A.; Craighead, K. L.; Gould, R. A. T.; Krogstad, D. A.; Wiley, J. S. *Coord. Chem. Rev.* **1995**, *143*, 219.

(7) (a) Albano, V. G.; Demartin, F.; Iapalucci, M. C.; Laschi, F.; Longoni, G.; Sironi, A.; Zanello, P. *J. Chem. Soc., Dalton Trans*. **1991**, 739. (b) Albano, V. G.; Demartin, F.; Iapalucci, M. C.; Longoni, G.; Sironi, A.; Zanotti, V. *J. Chem. Soc. Chem. Commun.* **1990**, 547. (c) Albano, V. G.; Demartin, F.; Iapalucci, M. C.; Longoni, G.; Monan, M.; Zanello, P. *J. Chem. Soc., Dalton Trans*. **1992**, 497. (d) Albano, V. G.; Demartin, F.; Iapalucci, M. C.; Longoni, G.; Monan, M.; Zanello, P., Sironi, A. *J. Chem. Soc., Dalton Trans*. **1993**, 173. (e) Ceriotti, A.; Demartin, F.; Heaton, B. T.; Ingallina, P.; Longoni, G.; Manassero, N.; Marchionna, M.; Masciocchi, N. *J. Chem. Soc., Chem. Commun.* **1989**, 786.

(8) Vidal, J. L.; Troup, J. M. *J. Organomet. Chem.* **1981**, *213*, 351.

(9) (a) Briant, C. E.; Theobald, B. R. C.; White, J. W.; Bell, L. K.; Mingos, D. M. P. *J. Chem. Soc., Chem. Commun.* **1981**, 201. (b) Briant C. E.; Hall, K. V.; Mingos, D. M. P. *J. Chem. Soc., Chem. Commun.* **1984**, 290. (c) Copley, R. C. B.; Mingos, D. M. P. *J. Chem. Soc., Dalton Trans.* **1992**, 1755. (d) B. K. Teo, H. Dang, H. Zhang, as quoted in: Zhang, H.; Teo, B. K. *Inorg. Chim. Acta* **1997**, *265*, 213.

(10) (a) Rieck, D. F.; Gavney, J. A., Jr.; Norman, R. L.; Hayashi, R. K.; Dahl, L. F. *J. Am. Chem. Soc.* **1992**, *114*, 10369. (b) Rieck, D. F.; Montag, R. A.; McKechnie, T. S.; Dahl, L. F. *J. Am. Chem. Soc.* **1986**, *108*, 1330. (c) DesEnfants, R. E., II; Gavney, J. A., Jr.; Hayashi, R. K.; Dahl, L. F. *J. Organomet. Chem.* **1990**, *383*, 543. (d) Zebrowski, J. P.; Hayashi, R. K.; Dahl, L. F. *J. Am. Chem. Soc.* **1993**, *115*, 1142. (e) Kahaian, A. J.; Thoden, J. B.; Dahl, L. F., *J. Chem. Soc., Chem. Commun.* **1992**, 353.

(11) (a) Teo, B. K.; Keating, K. *J. Am. Chem. Soc.* **1984**, *106*, 2224. (b) Teo, B. K.; Zhang, H.; Shi, X. *Inorg. Chem.* **1990**, *29*, 2083. (c) Teo, B. K.; Shi, X.; Zhang, H. *J. Am. Chem. Soc.* **1991**, *113*, 4329. (d) Teo, B. K.; Zhang, H. *Angew. Chem., Int. Ed. Engl.* **1992**, *31*, 445. (e) Teo, B. K.; Shi, X.; Zhang, H. *J. Chem. Soc., Chem. Commun.* **1992**, 1195. (f) Teo, B. K.; Shi, X.; Zhang, H. *J. Cluster Sci.* **1993**, *4* (4), 471. (g) Teo, B. K.; Zhang, H. *Inorg. Chem.* **1991**, *30*, 3115. (h) Teo, B. K.; Zhang, H.; Shi, X. *J. Am. Chem. Soc.* **1990**, *112*, 8552. (i) Teo, B. K.; Hong, M.; Zhang, H.; Huang, D.; Shi, X. *J. Chem. Soc., Chem. Commun.* **1988**, 204. (j) Teo, B. K.; Hong, M.; Zhang, H.; Huang, D. *Angew. Chem., Int. Ed. Engl.* **1987**, *26*, (6), 897. (k) Teo, B. K.; Shi, X.; Zhang, H. *Inorg. Chem.* **1993**, *32*, 3987. (l) B. K. Teo, X. Shi, H. Zhang, cited in *Chem. Eng. News* **1989**, *67*, 6. (m) Teo, B. K.; Zhang, H. *Coord. Chem. Rev.* **1995**, *143*, 611.

S0020-1669(98)00006-8 CCC: $15.00
Published on Web 04/30/1998

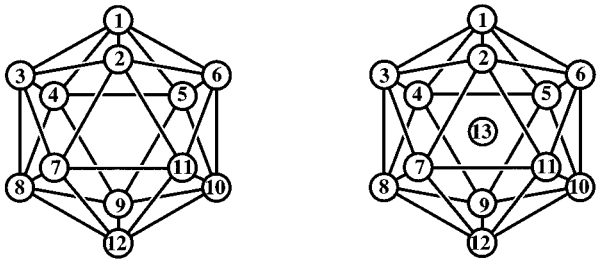

Figure 1. Numbering scheme for noncentered (a) and centered (b) icosahedra.

atoms. Furthermore, the icosahedron has emerged as basic units in solid-state materials such as several allotropes of boron,[12] complex borides,[13] gallides,[14] and quasicrystalline aluminum alloys.[15] Hence, it is of prime importance to understand the structure and bonding of multimetallic clusters based on the icosahedral framework.

An icosahedron can be either noncentered or centered, as illustrated in Figure 1. There are many stereoisomers (or *polytypes* in mathematical terminology) for a noncentered (12-atom) or a centered (13-atom) icosahedral cluster consisting of two types of atoms. In an earlier paper,[16] we enumerated all such possible stereoisomers of a binary icosahedral (either noncentered or centered) cluster via Polya's theorem. While the numbers of *achiral* and *chiral* stereoisomers for a given combination of the two types of atoms (or two colors in mathematical terms) A and B may be determined via Polya's theorem,[17,18] the actual structures are not readily available. This paper provides a complete iconography of all possible stereoisomers of a binary icosahedron (a total of 96 for noncentered and 192 for centered icosahedra) by utilizing a simple symmetry-based algorithm. This constitutes the first part of this paper.

The second part of this paper deals with the relative stabilities of these stereoisomers for a given combination of A and B atoms, which is important to the site preference problem in multimetallic systems, including mixed-metal clusters, metal alloy systems, multimetallic catalysts, etc. While site preference is a manifestation of the various and often competing bonding effects, we shall focus our attention on the metal−metal interactions in this paper. A simple theory capable of providing a relative measure of bond strengths of various metal−metal interactions in a metal cluster is reported herein. The theory is based on the Lennard-Jones potential and cohesive energies of transition metals. The sum of all pairwise metal−metal bond energies in a metal cluster of a given structure and metal combination then provides a measure of the relative stabilities of various stereoisomers. We shall illustrate the utility of this simple theory by applying it to *all possible stereoisomers* of binary icosahedral clusters containing the Au−Ag, Au−Ni, and Au−Pt combinations. On the basis of the calculated energies, two simple rules—the Strong-Bond rule and the Hetero-Bond rule—were formulated. These rules are useful in predicting the relative stabilities of these stereoisomers. We believe that the theory and the methodologies described in this paper, as well as the site preference rules deduced from these model calculations, can also be applied to other mixed-metal polyhedral cluster systems.

Table 1. Numbers (Z) of All Possible Stereoisomers of Noncentered and Centered Binary Icosahedral Clusters under I or I_h[a] Point Group Symmetry As Predicted by Polya's Theorem

noncentered		centered			
formulas	Z	formulas	B-centered	A-centered	Z
		B_{13}	1		1
B_{12}	1	AB_{12}	1	1	2
AB_{11}	1	A_2B_{11}	3	1	4
A_2B_{10}	3	A_3B_{10}	5	3	8
A_3B_9	5	A_4B_9	12(10)	5	17(15)
A_4B_8	12(10)	A_5B_8	14(12)	12(10)	26(22)
A_5B_7	14(12)	A_6B_7	24(18)[c]	14(12)	38(30)
A_6B_6	24(18)[b]	B_6A_7	14(12)	24(18)[c]	38(30)
B_5A_7	14(12)	B_5A_8	12(10)	14(12)	26(22)
B_4A_8	12(10)	B_4A_9	5	12(10)	17(15)
B_3A_9	5	B_3A_{10}	3	5	8
B_2A_{10}	3	B_2A_{11}	1	3	4
BA_{11}	1	BA_{12}	1	1	2
A_{12}	1	A_{13}		1	1
$\Sigma =$	96(82)	$\Sigma =$	96(82)	96(82)	192(164)[d]

[a] Results for I_h symmetry, if different from I symmetry, are given in the parentheses. [b] Note the symmetrical nature of the numbers of stereoisomers (with respect to the A_6B_6 set) as a result of A↔B "atom inversion" for noncentered binary icosahedra (i.e. A_nB_{12-n} has the same number of stereoisomers as B_nA_{12-n}). The A_6B_6 stereoisomers "invert" into the same set (see text). [c] For centered binary icosahedra, the B-centered A_nB_{13-n} set "inverts" into the A-centered B_nA_{13-n} set. [d] Note the typographical error of the number 192 in Table III of ref 16.

II. Iconography of Stereoisomers of a Binary Icosahedral Cluster

In a previous paper,[16] we used Polya's theorem[17,18] to calculate the numbers of all possible stereoisomers (polytypes) of a binary (two-colored) icosahedron, either noncentered or centered, as summarized in Table 1. In this paper, we report the complete iconography (Chart 1 and Table 2) of all possible stereoisomers for a given combination of A and B atoms. The following introductory remarks are necessary for later discussions.

(A) Nomenclature and The Numbering System. The IUPAC numbering system for an icosahedron is depicted in Figure 1. In this paper, the center atom is labeled as 13. Each stereoisomer is represented by an array of numbers (hereafter referred to as *indices*) preceding the chemical formula. The indices indicate the "minority" atom sites. The chemical formula follows the general convention of listing the positions of the minority atoms first. For example, 1, 7, 13-Pt_3Au_{10} indicates a centered icosahedral gold-rich cluster with three Pt atoms occupying positions 1, 7 (surface), and 13 (center).

To avoid ambiguities in naming the stereoisomers, the lowest possible consecutive indices are chosen for the minority atoms. For example, 1,2,4,11-A_4B_9 is preferred over 1,2,5,9-A_4B_9 since each consecutive number is the lowest possible number, though both denote the exact same cluster. Similarly, 1,2,8,12-A_4B_9

(12) Hoard, J. L.; Hughes, R. E. In *The Chemistry of Boron and Its Compounds*; Muetterties, E. L., Ed.; John Wiley & Sons: New York, 1967; p 25.
(13) Emin, D.; Aselage, T.; Beckel, C. L.; Howard, I. A.; Wood, C. (Eds.) *Boron-Rich Solids*; American Institute of Physics Conference Proceedings 140, American Institute of Physics: New York, 1986.
(14) (a) Belin, C. *Acta Crystallogr.* **1981**, *B37*, 2060. (b) Belin, C. *Acta Crystallogr.* **1980**, *B36*, 1339.
(15) (a) Levine, D.; Steinhardt, P. J. *Phys. Rev. Lett.* **1984**, *53*, 2477. (b) Levine, D.; Steinhardt, P. J. *Phys. Rev. B* **1986**, *34*, 596.
(16) Teo, B. K.; Zhang, H.; Kean, Y.; Dang, H.; Shi, X. *J. Chem. Phys.* **1993**, *99*, 2929.
(17) (a) Polya, G. *Acta Math.* **1937**, *68*, 145. (b) De Bruijn, N. G. *Niew. Arch. Wiskde.* **1971**, *19*, 89.
(18) (a) McLarnan, T. J. *J. Solid State Chem.* **1978**, *26*, 235. (b) Moore, P. B. *Neue J. Jahrb. Miner. Abh.* **1974**, *120*, 205. (c) Burdett, J. K. *Inorg. Chem.* **1975**, *14*, 375. (d) Burdett, J. K. In *Advances in Chemical Physics* Prigogine, I., Rice, S., Eds.; John Wiley & Sons: New York, 1982; Vol. 49.

Chart 1. Iconography of Icosahedra: All Possible Stereoisomers of A_nB_{12-n} Noncentered Icosahedral Clusters[a]

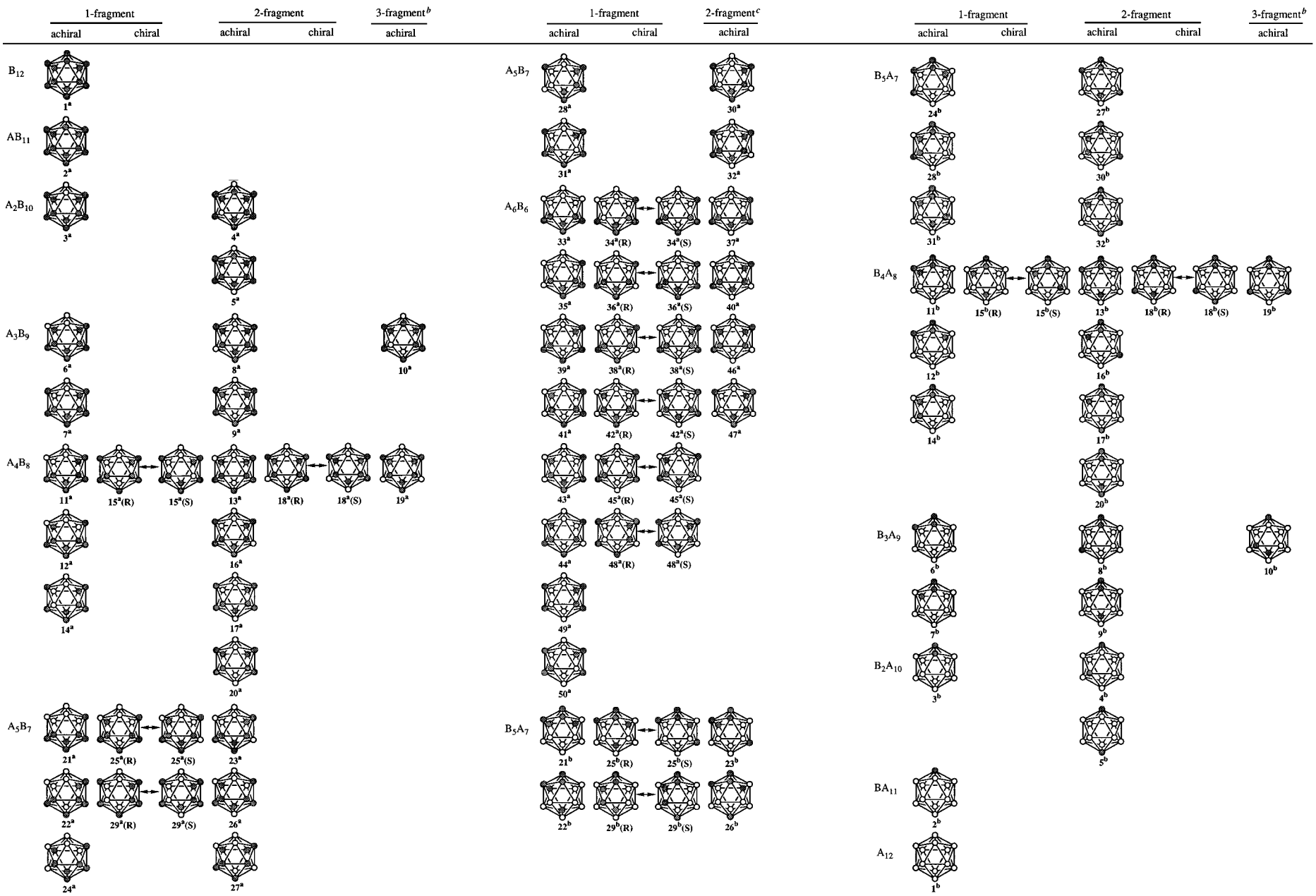

[a] A in white and B in black; chiral pairs are designated by double arrows. [b] No entries for "3-fragment, chiral". [c] No entries for "3 fragment" or for "2-fragment, chiral".

Table 2. Designators, Nomenclatures, Numbers of Minority and Majority Fragments, and Point Group Symmetries of All Possible Stereoisomers of Noncentered Binary Icosahedral Clusters[a]

				fragments		
designator	nomenclature	designator	nomenclature	minority	majority	point group
1[a]	B_{12}	**1**[b]	A_{12}	1	1	I_h
2[a]	1-AB_{11}	**2**[b]	1-BA_{11}	1	1	C_{5v}
3[a]	1,2-A_2B_{10}	**3**[b]	1,2-B_2A_{10}	1	1	C_{2v}
4[a]	1,7-A_2B_{10}	**4**[b]	1,7-B_2A_{10}	2	1	C_{2v}
5[a]	1,12-A_2B_{10}	**5**[b]	1,12-B_2A_{10}	2	1	D_{5d}
6[a]	1,2,3-A_3B_9	**6**[b]	1,2,3-B_3A_9	1	1	C_{3v}
7[a]	1,2,4-A_3B_9	**7**[b]	1,2,4-B_3A_9	1	1	C_s
8[a]	1,2,8-A_3B_9	**8**[b]	1,2,8-B_3A_9	2	1	C_s
9[a]	1,2,9-A_3B_9	**9**[b]	1,2,9-B_3A_9	2	1	C_s
10[a]	1,7,9-A_3B_9	**10**[b]	1,7,9-B_3A_9	3	1	C_{3v}
11[a]	1,2,3,4-A_4B_8	**11**[b]	1,2,3,4-B_4A_8	1	1	C_{2v}
12[a]	1,2,3,5-A_4B_8	**12**[b]	1,2,3,5-B_4A_8	1	1	C_s
13[a]	1,2,3,9-A_4B_8	**13**[b]	1,2,3,9-B_4A_8	2	1	C_s
14[a]	1,2,4,7-A_4B_8	**14**[b]	1,2,4,7-B_4A_8	1	1	C_s
15[a]**(R)**	1,2,4,9-A_4B_8	**15**[b]**(R)**	1,2,4,9-B_4A_8	1	1	C_2
16[a]	1,2,4,10-A_4B_8	**16**[b]	1,2,4,10-B_4A_8	2	1	C_s
15[a]**(S)**	1,2,4,11-A_4B_8	**15**[b]**(S)**	1,2,4,11-B_4A_8	1	1	C_2
17[a]	1,2,4,12-A_4B_8	**17**[b]	1,2,4,12-B_4A_8	2	1	C_2
18[a]**(R)**	1,2,8,9-A_4B_8	**18**[b]**(R)**	1,2,8,9-B_4A_8	2	1	C_2
19[a]	1,2,8,10-A_4B_8	**19**[b]	1,2,8,10-B_4A_8	3	1	C_{2v}
18[a]**(S)**	1,2,8,12-A_4B_8	**18**[b]**(S)**	1,2,8,12-B_4A_8	2	1	C_2
20[a]	1,2,9,12-A_4B_8	**20**[b]	1,2,9,12-B_4A_8	2	1	D_{2h}
21[a]	1,2,3,4,5-A_5B_7	**21**[b]	1,2,3,4,5-B_5A_7	1	1	C_s
22[a]	1,2,3,4,9-A_5B_7	**22**[b]	1,2,3,4,9-B_5A_7	1	1	C_s
23[a]	1,2,3,4,10-A_5B_7	**23**[b]	1,2,3,4,10-B_5A_7	2	1	C_s
24[a]	1,2,3,5,8-A_5B_7	**24**[b]	1,2,3,5,8-B_5A_7	1	1	C_s
25[a]**(R)**	1,2,3,5,9-A_5B_7	**25**[b]**(R)**	1,2,3,5,9-B_5A_7	1	1	C_1
25[a]**(S)**	1,2,3,4,10-A_5B_7	**25**[b]**(S)**	1,2,3,4,10-B_5A_7	1	1	C_1
26[a]	1,2,3,5,12-A_5B_7	**26**[b]	1,2,3,5,12-B_5A_7	2	1	C_s
27[a]	1,2,3,9,10-A_5B_7	**27**[b]	1,2,3,9,10-B_5A_7	2	1	C_s
28[a]	1,2,4,7,8-A_5B_7	**28**[b]	1,2,4,7,8-B_5A_7	1	2	C_{5v}
29[a]**(R)**	1,2,4,7,9-A_5B_7	**29**[b]**(R)**	1,2,4,7,9-B_5A_7	1	1	C_1
30[a]	1,2,4,7,10-A_5B_7	**30**[b]	1,2,4,7,10-B_5A_7	2	1	C_s
29[a]**(S)**	1,2,4,7,12-A_5B_7	**29**[b]**(S)**	1,2,4,7,12-B_5A_7	1	1	C_1
31[a]	1,2,4,9,11-A_5B_7	**31**[b]	1,2,4,9,11-B_5A_7	1	1	C_s
32[a]	1,2,4,10,12-A_5B_7	**32**[b]	1,2,4,10,12-B_5A_7	2	1	C_s
33[a]	1,2,3,4,5,6-A_6B_6	**33**[b] = **33**[a]		1	1	C_{5v}
34[a]**(R)**	1,2,3,4,5,7-A_6B_6	**34**[b]**(R)** = **34**[a]**(R)**		1	1	C_1
35[a]	1,2,3,4,5,8-A_6B_6	**35**[b] = **35**[a]		1	1	C_{3v}
34[a]**(S)**	1,2,3,4,5,9-A_6B_6	**34**[b]**(S)** = **34**[a]**(S)**		1	1	C_1
36[a]**(R)**	1,2,3,4,5,10-A_6B_6	**36**[b]**(R)** = **36**[a]**(R)**		1	1	C_1
36[a]**(S)**	1,2,3,4,5,11-A_6B_6	**36**[b]**(S)** = **36**[a]**(S)**		1	1	C_1
37[a]	1,2,3,4,5,12-A_6B_6	**37**[b] = **41**[a]		2	1	C_s
38[a]**(R)**	1,2,3,4,9,10-A_6B_6	**38**[b]**(R)** = **38**[a]**(R)**		1	1	C_1
39[a]	1,2,3,4,9,11-A_6B_6	**39**[b] = **44**[a]		1	1	C_{2v}
38[a]**(S)**	1,2,3,4,9,12-A_6B_6	**38**[b]**(S)** = **38**[a]**(S)**		1	1	C_1
40[a]	1,2,3,4,10,12-A_6B_6	**40**[b] = **49**[a]		2	1	C_{2v}
41[a]	1,2,3,5,8,9-A_6B_6	**41**[b] = **37**[a]		1	2	C_s
42[a]**(R)**	1,2,3,5,8,10-A_6B_6	**42**[b]**(R)** = **42**[a]**(R)**		1	1	C_1
43[a]	1,2,3,5,8,11-A_6B_6	**43**[b] = **43**[a]		1	1	C_{3v}
42[a]**(S)**	1,2,3,5,8,12-A_6B_6	**42**[b]**(S)** = **42**[a]**(S)**		1	1	C_1
44[a]	1,2,3,5,9,10-A_6B_6	**44**[b] = **39**[a]		1	1	C_{2v}
45[a]**(R)**	1,2,3,5,9,12-A_6B_6	**45**[b]**(R)** = **45**[a]**(R)**		1	1	C_1
45[a]**(S)**	1,2,3,5,10,12-A_6B_6	**45**[b]**(S)** = **45**[a]**(S)**		1	1	C_1
46[a]	1,2,3,9,10,12-A_6B_6	**46**[b] = **50**[a]		2	1	D_{3d}
47[a]	1,2,4,7,8,10-A_6B_6	**47**[b] = **47**[a]		2	2	C_{5v}
48[a]**(R)**	1,2,4,7,9,10-A_6B_6	**48**[b]**(R)** = **48**[a]**(R)**		1	1	C_1
49[a]	1,2,4,7,9,12-A_6B_6	**49**[b] = **40**[a]		1	2	C_{2v}
48[a]**(S)**	1,2,4,7,10,12-A_6B_6	**48**[b]**(S)** = **48**[a]**(S)**		1	1	C_1
50[a]	1,2,4,9,11,12-A_6B_6	**50**[b] = **46**[a]		1	2	D_{3d}

[a] The formal "atom-inversion" process involves interchanging atom types A and, B, hence A_nB_{12-n} (columns 1 and 2) becomes B_nA_{12-n} (columns 3 and 4) and the designator D^a (where atom type A is minority) becomes D^b (where atom type B is minority). Note that A_6B_6 stereoisomers invert into the same set. See text for other details.

is preferred over 1,2,9,10-A_4B_9. In this manner, each stereoisomer is uniquely defined. A computer program based on a simple symmetry algorithm was used to generate all possible stereoisomers. The results for noncentered icosahedral clusters are listed in Chart 1 and Table 2. Each stereoisomer is further denoted by a designator D_j^i (see Chart 1 and Table 2). The designator consists of a number, *D*, which represents the order of the stereoisomer in Table 2, with a superscript *i* indicating the kind of minority atoms and a subscript *j* indicating the type of central atom. For example, $5_A{}^a$ in Table 2 designates the stereoisomer 1,12,13-A_3B_{10} with A as minority atoms (at positions 1 and 12) and it is A-centered (at position 13).

(B) Noncentered Icosahedral Clusters. As tabulated in Table 1,[16] we have applied Polya's enumeration theorem[17,18] to a noncentered binary icosahedral cluster under noncentrosymmetric *I* symmetry or centrosymmetric I_h symmetriy. Under *I* symmetry, there are 68 achiral structures and 28 chiral structures (14 chiral pairs). The number *Z* represents all possible structures for a noncentered icosahedral cluster with n_a atoms of type A and n_b atoms of type B. Note that $n_a + n_b = 12$ for a noncentered icosahedron. The iconography of all possible stereoisomers of a noncentered binary icosahedral cluster is portrayed in Chart 1. The nomenclature of the stereoisomers, along with the designators, the numbers of fragments of minority and majority atoms, and the point group symmetries are listed in Table 2. The importance of the fragment information will be discussed later.

For I_h symmetry, the *inversion symmetry* (*i*) eliminates one partner of each chiral pair, giving rise to 68 achiral structures and 14 chiral structures. These results are also listed in Table 1 (in parentheses).

In Chart 1 and Table 2, the chiral pairs are denoted by the same designator but with an R or S in parentheses. They are further indicated by double arrows in Chart 1. The symbols R and S carry no special meaning except that the one with lower indices is denoted by R.

(C) Centered Icosahedral Clusters. For a centered icosahedron, the nuclearity is $n_a' + n_b' = 13$ where n_a' and n_b' are the numbers of atoms of type A and type B, respectively. Here the primes designate that it is a centered icosahedral structure.

Table 1 also gives the structure counts for centered icosahedra.[16] Here, the addition of a type B atom to the center of the noncentered icosahedron produces a B-centered icosahedron with $n_a' = n_a$ and $n_b' = n_b + 1$ (i.e. n_b increases by 1). The numbers of structures (Z_B) can be derived from the appropriate column for the noncentered icosahedron in Table 1. Similarly, an A-centered icosahedron has $n_a' = n_a + 1$ and $n_b' = n_b$ (i.e. n_a increases by 1). The numbers of structures (Z_A) under this category can also be derived accordingly from the corresponding column for the noncentered icosahedron in Table 1. The total number of structures, $Z' = Z_A + Z_B$, for each combination of n_a' and n_b' is given in the last column of Table 1.

Under *I* symmetry, there are a total of 192 stereoisomers, whereas under I_h symmetry, the inversion symmetry reduces the structure count to 164 stereoisomers (in parentheses). The iconography of all possible stereoisomers of either an A- or a B-centered icosahedral cluster can be obtained from Chart 1 by adding an A or a B atom to the center (the 13th position) of the icosahedron. One example is given in Figure 2. In this example, the addition of an A or a B atom to the center of the noncentered icosahedral cluster 1,12-A_2B_{10} (5^a) produces centered icosahedral clusters 1,12,13-A_3B_{10} ($5_A{}^a$) or 1,12-A_2B_{11} ($5_B{}^a$), respectivety. Similarly, adding an A or a B atom to the center of the noncentered icosahedral cluster 1,12-B_2A_{10} (5^b) gives rise to the centered icosahedral clusters 1,12-B_2A_{11} ($5_A{}^b$) and 1,12,13-B_3A_{10} ($5_B{}^b$), respectivety.

III. Metallic Bond Energy (MBE) Calculations

(A) Metal−Metal Bond Strength. Recently we suggested the use of bond strength vs charge accumulation (BSCA) plots for the determination of site preference in mixed-metal clusters.[19] In this paper, we focus our attention on the bond strength since actual charges on each metal site cannot be accurately assessed without detailed molecular orbital calculations. This assumption is reasonable due to the fact that bond strengths are, generally speaking, more important than charge accumulation for transition metal clusters in the assessment of the relative stabilities of various stereoisomers. For main-group clusters or for mixed transition-metal/main-group clusters, however, both factors may need to be taken into account.

There are two major contributions to the bond energy of a metal−metal bond[20,21]—covalent and ionic—which we shall discuss next.

Covalent Contribution. The covalent contribution to the bond energy (ϵ) of a homonuclear metal−metal (A−A) bond can be estimated from the cohesive energy (or, equivalently, the heat of atomization, ΔH°_{298}) of the metal.[22] For example, for face-centered cubic (fcc) or hexagonal close-packing (hcp) metals, the following bond energy expression may be used:

$$\epsilon_{AA} = \Delta H^\circ_{298}/6 \tag{1a}$$

The factor $^1/_6$ is due to the fact that there are 12 nearest neighbors in a fcc (or hcp) metal which is overcounted by a factor of 2.[23,24] For body-centered cubic (bcc) metals with eight nearest neighbors and six next-nearest neighbors, a somewhat different expression may be more appropriate:[24]

$$\epsilon_{AA} = \Delta H^\circ_{298}/5.548 \tag{1b}$$

The covalent contribution to the bond energy of a heteronuclear bond is more difficult to calculate due to the paucity of experimental results. Furthermore, they are quite sensitive to the chemical environment. Nevertheless, we can use simple arithmatic (eq 2a) or geometric (eq 2b) means of the corresponding homonuclear bonds (A−A and B−B) to estimate the bond energy of a heteronuclear (A−B) bond, as follows

$$\epsilon_{AB} = {}^1/_2(\epsilon_{AA} + \epsilon_{BB}) \tag{2a}$$

or

$$\epsilon_{AB} = (\epsilon_{AA}\epsilon_{BB})^{1/2} \tag{2b}$$

Throughout this paper, we shall use eq 2a.

Ionic Contribution. A covalent bond can have *ionic character*, due to the disparity of the electronegativities of the constituents, providing extra stabilization energy to the bond. The gain in bond energy due to the ionic character can be estimated from the following equations.

$$(\epsilon_{AB})_{ion} = 23[(\chi_A - \chi_B)/3]^2 \text{ kcal/mol}, \quad \text{for fcc or hcp structure} \tag{3a}$$

$$(\epsilon_{AB})_{ion} = 23[(\chi_A - \chi_B)/2.774]^2 \text{ kcal/mol}, \quad \text{for bcc structure} \tag{3b}$$

Here χ is Pauling's electronegativity.[25] These equations are in accord with Pauling's equation for heteronuclear bonds involving main-group elements with some modification. Specifically, the modification involves a factor of 3 (for fcc and hcp metals) or 2.774 (for bcc metals) in the estimates of differences in electronegativities between different metals. This is a reasonable assumption due to the fact that, in general, main-group elements normally have a maximum coordination number of 4 (sp^3), whereas transition metals, in the case of fcc or hcp structures,

(19) Teo, B. K.; Zhang, H.; Shi, X. *Inorg. Chem.* **1994**, *33*, 4086.

(20) Arguments have been put forth independently by Anderson, Burdett, and Czech[21a] and by Allen and Capitani[21b] that the term "metallic bond" is fully encompassed by the concept of covalent bonding.

(21) (a) Anderson, W. P.; Burdett, J. K.; Czech, P. T. *J. Am. Chem. Soc.* **1994**, *116*, 8808. (b) Allen, L. C.; Capitani, J. F. *J. Am. Chem. Soc.* **1994**, *116*, 8810.

(22) Kerr, J. A. In *CRC Handbook of Chemistry and Physics*, 65th ed.; CRC Press: Boca Raton, FL, 1985; F-181.

(23) Wooley, R. G. In Transition Metal Clusters; Johnson, B. F. G., Ed.; Wiley: Chichester, U.K., 1980, p 607.

(24) Housecroft, C. E.; Wade, K. *J. Chem. Soc. Chem. Commun.* **1978**, 765.

(25) Pauling, L. *The Nature of the Chemical Bond*, 3rd ed.; Cornell University Press: Ithaca, NY, 1960.

have a maximum coordination number of 12. Hence, the effect of the difference in electronegativities (in terms of the ionic contribution to the bond energy) for each heterometallic bond should be "diluted" by a factor of 4/12 = 1/3 (i.e., spread out over 12 bonds rather than 4 bonds).[26] Our experience with other more elaborate factors or schemes for estimating the extra stabilization energy due to ionicity indicates that this simple modification of Pauling's equation is adequate and the results are quite reasonable.

Metal−Metal Bond Energy. The metallic bond energy of a heteronuclear bond A−B (in kcal/mol) is then given by the sum of *covalent* and *ionic* contributions:

$$\epsilon_{AB} = 1/2(\epsilon_{AA} + \epsilon_{BB}) + 23[(\chi_A - \chi_B)/3]^2 \text{ for fcc or hcp metals} \quad (4a)$$

$$\epsilon_{AB} = 1/2(\epsilon_{AA} + \epsilon_{BB}) + 23[(\chi_A - \chi_B)/2.774]^2 \text{ for bcc metals} \quad (4b)$$

For a homonuclear bond, eq 1 should be used. The ϵ and χ values used for groups 10 and 11 metals in our calculations are listed in the Appendix.

(B) Energy Minimization and Structure Optimization. As a first approximation, the sum of bond energies due to all pairwise interactions between the atoms provides a measure of the relative stabilities of various stereoisomers of a metal cluster with a given structure and metal combination. In this paper, we have explored the validity of this hypothesis by using a Lennard-Jones potential and cohesive energy to model the pairwise interactions among metal atoms.

Lennard-Jones Potential: Pairwise Interactions. In our calculations, the pairwise interactions of the metal−metal bonds are modeled by the Lennard-Jones potential, as follows:

$$U_{ij}(r_{ij}) = 4\epsilon_{ij}[(\sigma/r_{ij})^{12} - (\sigma/r_{ij})^6] \quad (5)$$

where ϵ is the bond energy calculated based on eq 1 and eq 4; σ is the intercept on the abscissa of the $U_{ij}(r_{ij})$ vs r_{ij} plot. The parameter σ is related to the *equilibrium distance*, d_{ij}, between two metal atoms by $\sigma = d_{ij}/2^{1/6}$. In fact, at the equilibrium distance, $r_{ij} = d_{ij}$, the potential is equal to the negative of the metallic bond energy, $U_{ij}(d_{ij}) = -\epsilon_{ij}$. For a homonuclear bond, we take d_{ij} as the nearest neighbor distance in the crystal structure. For a heteronuclear bond, the equilibrium distance d is taken as the simple arithmatic mean of the corresponding distances of the two constituent metals:

$$d_{AB} = (d_{AA} + d_{BB})/2 \quad (6)$$

Here d_{AA} and d_{BB} are the nearest neighbor distances in the crystal structures of metals A and B, respectively.

Total Metallic Bond Energy. We now define a total metallic bond energy, U_m, as the sum of bond energies, U_{ij}, between atoms i and j, for all pairwise metal−metal interactions:

$$U_m = {}^1/_2\sum U_{ij} \quad (7)$$

The factor of $^1/_2$ arises from the overcount of the pairwise interactions. The "optimized structure" for each stereoisomer is then obtained by minimizing the total metallic bond energy U_m with respect to all interatomic distances r_{ij}. The minimized total metallic bond energies U_m are tabulated in Table 3 for all stereoisomers of three model binary mixed-metal (Au−Ag, Au−Ni, and Au−Pt) icosahedral cluster systems based on the ϵ and χ values listed in the Appendix. These three bimetallic systems were chosen because of their disparities in cohesive energy (in the order Pt > Ni > Au > Ag) as well as their tendency to form icosahedral clusters. These minimized "total metallic bond energies" provide a measure of the *relative stability* of the stereoisomers for the A_nB_{13-n} icosahedral clusters. The most stable structures are indicated by asterisks (*) in Table 3.

(26) For bcc metals, a somewhat different value should be used since there are eight nearest neighbors and six next-nearest neighbors. The value should be $4/(2 \times 5.548) = 4/11.096 = 1/2.774$, as per ref 24.

(C) Calculations. All calculations were performed on Silicon Graphics Personal IRIS computer using a modified version of the MOIL program,[27] incorporating eqs 4−7. MOIL is a package of general-purpose computer programs for molecular dynamics simulations. For the present work, however, only the energy minimization routines were used. Each metal atom in a cluster is treated as a "monomer", and the cluster as a whole is an ensemble of "monomers" interacting via pairwise Lennard-Jones potentials. No charges were assigned to the metal atoms (i.e., they were all treated as neutral entities). The total metallic energy of each cluster was minimized by varying the interatomic distances. Though the energy-minimized clusters showed some distortions from the ideal icosahedral geometry, the resulting interatomic distances (a total of 42) do not deviate substantially from the values given by eq 6 and hence will not be reported here.

IV. Results and Discussions

(A) Iconography of Icosahedral Clusters. The complete iconography of all possible stereoisomers of noncentered binary A_nB_{12-n} icosahedral clusters is presented in Chart 1. The nomenclatures of these stereoisomers, based on a unique numbering system consistent with the IUPAC rule, are listed in Table 2, along with the numbers of fragments of minority and majority atoms and the point group symmetries. The iconography of all possible stereoisomers of A- or B-centered binary A_nB_{13-n} icosahedral clusters can be obtained from Chart 1 by adding an A or a B atom to the center (the 13th position), as illustrated in Figure 2 and discussed earlier.

Enumeration and Determination of Stereoisomers. Although the numbers of stereoisomers, chiral vs achiral, noncentered vs A- or B-centered, can be enumerated via Polya's theorem (see results tabulated in Table 1), the actual structures cannot be determined easily. The actual structures were determined in this paper by taking into account the symmetry operations of the appropriate point group (60 or 120 symmetry operations for I or I_h point group, respectively), using a simple computer algorithm. The numbers of the resulting stereoisomers agree with those predicted by Polya's theorem. The results are depicted in Chart 1 and tabulated in Table 2.

Chiral Pairs. As shown in Chart 1 and Table 2, there are 14 chiral pairs for noncentered binary icosahedral clusters. Specifically, there are no chiral pairs for AB_{11}, A_2B_{10}, or A_3B_9 (nor for corresponding BA_{11}, B_2A_{10}, or B_3A_9); two chiral pairs each for A_4B_8 and A_5B_7 (and the corresponding B_4A_8 and B_5A_7); and six chiral pairs for A_6B_6. The same number doubles for centered icosahedral clusters, as stipulated in Table 1. The chiral pairs are denoted by R and S (in parentheses) bearing the same designator. They are further indicated by double arrows in Chart 1. For example, as depicted in Chart 1, the chiral pair 1,2,4,9-A_4B_8 and 1,2,4,11-A_4B_8 are designated by 15^a(R) and 15^a(S), respectively. The symbols R and S carry no special meaning except that the one with lower indices is denoted by R. As expected, chiral pairs have identical bonding energies (see Table 3).

Atom-Inversion. It can be seen from Table 1 that the number of stereoisomers, Z, is symmetrical with respect to $n_a = n_b = 6$. For example, there are three possible structures each for clusters with $n_a = 2$ and $n_b = 10$ (A_2B_{10}) and for clusters with $n_b = 2$ and $n_a = 10$ (B_2A_{10}). This is understandable since the numbers of stereoisomers remain the same even if the two types of atoms, A and B, are "interchanged". We shall refer to this as a formal "atom-inversion" process. One example, the inversion of 1,12-A_2B_{10} (5^a) into 1,12-B_2A_{10} (5^b), and the inversion of their centered derivatives is illustrated in Figure 2. In particular, the A-centered icosahedral cluster 1,12,13-A_3B_{10}

(27) Elber, R.; Roitberg, A.; Simmerling, C.; Goldstein, R.; Li, H. Y.; Verkhivker, G.; Keasar, C.; Zhang, J.; Ulitsky, A. *Comput. Phys. Commun.* **1995**, *91*, 159.

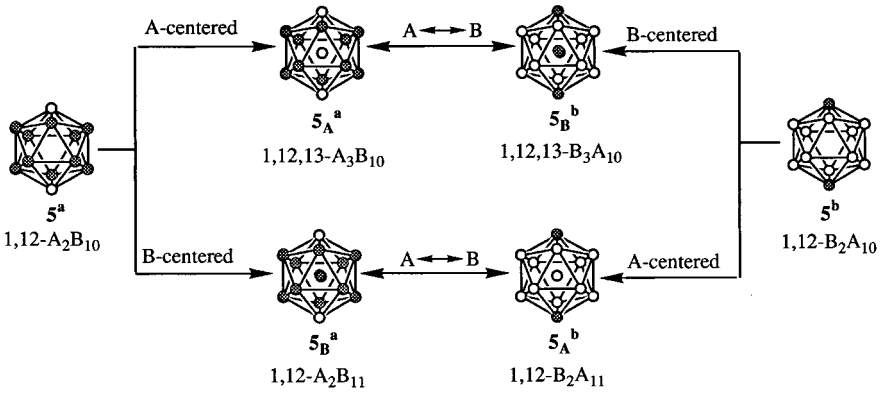

Figure 2. Examples of the generation of centered icosahedra from the corresponding noncentered icosahedra and the formal A ↔ B "atom-inversion" process (see text).

(5_A^a) "atom inverts" into the B-centered icosahedral cluster 1,-12,13-B_3A_{10} (5_B^b). Similarly, the B-centered icosahedral cluster 1,12-A_2B_{11} (5_B^a) "atom inverts" into the A-centered icosahedral cluster 1,12-B_2A_{11} (5_A^b).

A complete listing of stereoisomers of A_nB_{12-n} noncentered icosahedral clusters related by this formal "atom-inversion" process can be found in Table 2. The case of $n_a = n_b = 6$ (A_6B_6) is rather interesting and deserves some comments. Here the 24 stereoisomers form a set of structures that either "atom inverts" into another structure within the same set or "self-inverts" into itself (i.e., the same structure). This explains why there are no entries for B_6A_6 in Table 2. In fact, of the 24 stereoisomers in the A_6B_6 set, there are four pairs which are related by this "atom-inversion" process, while the remaining 16 structures self-invert into the same structure. For example, as illustrated in Figure 3, 1,2,3,4,10,12-A_6B_6 (40^a) "atom inverts" into 1,2,3,4,10,12-B_6A_6 (40^b), which can be renumbered as 1,2,4,7,9,12-A_6B_6 (49^a). By symmetry, it follows that 1,2,4,7,9,-12-B_6A_6 (49^b) = 1,2,3,4,10,12-A_6B_6 (40^a) "atom-inverts" into 1,2,3,4,10,12-B_6A_6 (40^b) = 1,2,4,7,9,12-A_6B_6 (49^a). Similarly, this atom-inversion process formally transforms 1,2,3,9,10,12-A_6B_6 (46^a) into 1,2,3,9,10,12-B_6A_6 (46^b), which can readily be renumbered as 1,2,4,9,11,12-A_6B_6 (50^a). On the other hand, some structures self-invert into themselves. For example, 1,2,4,7,8,10-A_6B_6 (47^a) "atom inverts" into 1,2,4,7,8,10-B_6A_6 (47^b), which can be renumbered as 1,2,4,7,8,10-A_6B_6 (47^a) (i.e., itself). Two more examples of "self-invertable" icosahedral clusters, 1,2,4,7,9,10-A_6B_6 (48^a(R)) and 1,2,4,7,10,12-A_6B_6 (48^a-(S)), are also shown in Figure 3.

An examination of Table 2 reveals that, in general, atom inversion does not alter the chirality of the structure. Here the word "chirality" refers to the R and S symbols used to denote the indices of the stereoisomers. In other words, for A_nB_{12-n} where $n \neq 6$, an achiral cluster always atom inverts into another achiral cluster (e.g., 1,2,4,7-A_4B_8 (14^a) into 1,2,4,7-B_4A_8 (14^b)), while a chiral cluster always atom inverts into another chiral cluster of the same handedness (e.g., 1,2,4,9-A_4B_8 (15^a(R)) into 1,2,4,9-B_4A_8 (15^b(R)) (see Table 2). Within the A_6B_6 subset, however, an achiral stereoisomer can either atom invert into a different achiral structure (e.g., 40^a into $40^b = 49^a$) or self-invert into the same structure (e.g., 47^a into $47^b = 47^a$) whereas a chiral stereoisomer always self-inverts into itself (e.g., 48^a(R) into 48^b(R) = 48^a(R)).

(B) Relative Stabilities of Stereoisomers. The calculated "total metallic bond energies" are tabulated in Table 3. A few remarks are warranted here.

Metal−Metal Interactions. The relative stabilities of different stereoisomers predicted in this paper are based solely on the calculated metallic bond energies. For systems where metal−ligand bonding becomes important, they must be included explicitly in the calculation (*vide infra*).

Energy Scaling. While the relative orders of the calculated "total metallic energies" are meaningful, the absolute energies can be "scaled" by multiplying all pairwise bond energies (A−A, B−B, A−B; cf. eq 4) by a common factor, without affecting the relative ordering of the stabilities.

Distance Scaling. Though we use eq 6, which is based on the nearest neighbor distances in bulk metals, to calculate the equilibrium distances in the Lennard-Jones potentials, we should point out that the results are quite insensitive to a "scaling" process whereby all the distances (d_{AA}, d_{BB}, d_{AB}) are modified by a common factor. In other words, the entire cluster can expand or contract to some extent without significantly affecting the *relative* ordering of the energetics of the various stereoisomers.

Fragments. The numbers of fragments of minority and majority atoms are presented in Chart 1 and Table 2. As shown in Table 2, *the maximum number of fragments on the surface of a binary icosahedral cluster is 3 for the minority atoms and 2 for the majority atoms*. We will make use of this fragment formation in the site preference discussion.

(C) Site Preference Rules. In theory, stereoisomers with higher total metallic bond energies (eq 7) should be thermodynamically more stable provided that the ligand bonding is not dominant (see Conclusion). There are two important contributions—covalent and ionic—to the "total metallic bonding energies". In this paper, these two bonding contributions are modeled by the two terms in eq 4. On the basis of the calculated bond energies tabulated in Table 3, two site preference rules—the Strong-Bond rule and the Hetero-Bond rule—can be formulated. These rules are extremely useful in ascertaining the relative stabilities of the stereoisomers, especially in the absence of calculations. They are also useful for understanding site preference in more complex structures built with binary icosahedral clusters as basic building blocks.

(1) Strong-Bond Rule: The Covalent Contribution. The Strong-Bond rule states that stereoisomers having a higher number of "strong bonds" tend to be more stable. Here the "strong bonds" are defined as metal−metal bonds with high metallic bonding energies. Strong bonds are generally formed by "strong metals" which have higher cohesive energies. The "Strong-Bond" rule stems from the *covalent* contribution to the metallic bonding energy. For example, as depicted in Scheme 1, of the two stereoisomers of the $AgAu_{12}$ icosahedral cluster, the Au-centered stereoisomer 1-$AgAu_{12}$ is more stable than the Ag-centered structure 13-$AgAu_{12}$ by 28.14 kcal/mol. This can be attributed to the fact that Au has a higher cohesive

Table 3. Calculated Total Metallic Energies of All Possible Stereoisomers for Centered Binary (Ag−Au, Ni−Au, and Pt−Au) Icosahedral Clusters[a]

B-centered				A-centered			
formulas	A = Ag B = Au	A = Ni B = Au	A = Pt B = Au	formulas	A = Ag B = Au	A = Ni B = Au	A = Pt B = Au
B_{13}	−650.27*	−650.27*	−650.27*				
1-AB_{12}	−645.74*	−659.36*	−675.48*	13-AB_{12}	−642.37*	−695.20*	−708.66*
1,2-A_2B_{11}	−639.31	−666.85	−700.41	1,13-A_2B_{11}	−636.06*	−707.71*	−734.14*
1,7-A_2B_{11}	−641.02	−667.46*	−700.45*				
1,12-A_2B_{11}	−641.14*	−667.14	−700.36				
1,2,3-A_3B_{10}	−630.99	−672.58	−725.08	1,2,13-A_3B_{10}	−627.85	−718.44	−759.33
1,2,4-A_3B_{10}	−632.69	−673.31	−725.11	1,7,13-A_3B_{10}	−629.55	−719.47*	−759.45*
1,2,8-A_3B_{10}	−634.40	−673.89	−725.15	1,12,13-A_3B_{10}	−629.67*	−719.24*	−759.40
1,2,9-A_3B_{10}	−634.51	−673.57	−725.06				
1,7,9-A_3B_{10}	−636.10*	−674.45*	−725.17*				
1,2,3,4-A_4B_9	−622.47	−677.32	−749.53	1,2,3,13-A_4B_9	−617.75	−727.20	−784.22
1,2,3,5-A_4B_9	−624.18	−677.99	−749.56	1,2,4,13-A_4B_9	−619.44	−728.43	−784.34
1,2,3,9-A_4B_9	−626.00	−678.23	−749.50	1,2,8,13-A_4B_9	−621.14	−729.44	−784.46
1,2,4,7-A_4B_9	−625.88	−678.70	−749.59	1,2,9,13-A_4B_9	−621.25	−729.22	−784.41
1,2,4,9-A_4B_9	−625.99	−678.38	−749.49	1,7,9,13-A_4B_9	−622.84*	−730.41*	−784.58*
1,2,4,10-A_4B_9	−627.58	−679.23	−749.60*				
1,2,4,11-A_4B_9	−625.99	−678.38	−749.49				
1,2,4,12-A_4B_9	−627.70	−678.93	−749.50				
1,2,8,9-A_4B_9	−627.70	−678.94	−749.53				
1,2,8,10-A_4B_9	−629.29*	−679.78*	−749.62				
1,2,8,12-A_4B_9	−627.70	−678.94	−749.53				
1,2,9,12-A_4B_9	−627.81	−678.64	−749.42				
1,2,3,4,5-A_5B_8	−613.77	−680.99	−773.76	1,2,3,4,13-A_5B_8	−607.45	−735.28	−808.95
1,2,3,4,9-A_5B_8	−615.58	−681.32	−773.68	1,2,3,5,13-A_5B_8	−609.14	−736.47	−809.06
1,2,3,4,10-A_5B_8	−617.29	−681.82	−773.69	1,2,3,9,13-A_5B_8	−610.95	−737.26	−809.13
1,2,3,5,8-A_5B_8	−617.17	−682.26	−773.78	1,2,4,7,13-A_5B_8	−610.83	−737.66	−809.18
1,2,3,5,9-A_5B_8	−617.29	−681.97	−773.70	1,2,4,9,13-A_5B_8	−610.94	−737.44	−809.12
1,2,3,5,10-A_5B_8	−617.29	−681.97	−773.70	1,2,4,10,13-A_5B_8	−612.53	−738.61	−809.29
1,2,3,5,12-A_5B_8	−618.99	−682.46	−773.69	1,2,4,11,13-A_5B_8	−610.94	−737.44	−809.12
1,2,3,9,10-A_5B_8	−619.10	−682.19	−773.63	1,2,4,12,13-A_5B_8	−612.64	−738.41	−809.23
1,2,4,7,8-A_5B_8	−617.17	−682.45	−773.80*	1,2,8,9,13-A_5B_8	−612.64	−738.44	−809.25
1,2,4,7,9-A_5B_8	−618.99	−682.65	−773.70	1,2,8,10,13-A_5B_8	−614.22*	−739.57*	−809.40*
1,2,4,7,10-A_5B_8	−620.57	−683.46	−773.80	1,2,8,12,13-A_5B_8	−612.64	−738.44	−809.25
1,2,4,7,12-A_5B_8	−618.99	−682.65	−773.70	1,2,9,12,13-A_5B_8	−612.75	−738.22	−809.19
1,2,4,9,11-A_5B_8	−619.10	−682.35	−773.59				
1,2,4,10,12-A_5B_8	−620.69*	−683.17*	−773.71				
1,2,3,4,5,6-A_6B_7	−603.17	−682.95	−797.73*	1,2,3,4,5,13-A_6B_7	−596.94	−742.62	−833.50
1,2,3,4,5,7-A_6B_7	−604.98	−683.24	−797.64	1,2,3,4,9,13-A_6B_7	−598.74	−743.58	−833.56
1,2,3,4,5,8-A_6B_7	−604.87	−683.52	−797.73*	1,2,3,4,10,13-A_6B_7	−600.44	−744.54	−833.67
1,2,3,4,5,9-A_6B_7	−604.98	−683.24	−797.64	1,2,3,5,8,13-A_6B_7	−600.32	−744.90	−833.72
1,2,3,4,5,10-A_6B_7	−606.68	−683.82	−797.63	1,2,3,5,9,13-A_6B_7	−600.43	−744.74	−833.67
1,2,3,4,5,11-A_6B_7	−606.68	−683.82	−797.63	1,2,3,5,10,13-A_6B_7	−600.43	−744.74	−833.67
1,2,3,4,5,12-A_6B_7	−608.39	−684.28	−797.62	1,2,3,5,12,13-A_6B_7	−602.13	−745.66	−833.77
1,2,3,4,9,10-A_6B_7	−608.50	−684.15	−797.54	1,2,3,9,10,13-A_6B_7	−602.24	−745.51	−833.74
1,2,3,4,9,11-A_6B_7	−608.50	−684.13	−797.51	1,2,4,7,8,13-A_6B_7	−600.32	−745.13	−833.72
1,2,3,4,9,12-A_6B_7	−608.50	−684.15	−797.54	1,2,4,7,9,13-A_6B_7	−602.13	−745.86	−833.77
1,2,3,4,10,12-A_6B_7	−610.20	−684.62	−797.56	1,2,4,7,10,13-A_6B_7	−603.71	−746.97*	−833.93*
1,2,3,5,8,9-A_6B_7	−608.38	−684.58	−797.65	1,2,4,7,12,13-A_6B_7	−602.13	−745.86	−833.77
1,2,3,5,8,10-A_6B_7	−610.09	−685.05	−797.63	1,2,4,9,11,13-A_6B_7	−602.24	−745.65	−833.71
1,2,3,5,8,11-A_6B_7	−609.97	−685.34	−797.73*	1,2,4,10,12,13-A_6B_7	−603.82*	−746.79	−833.89
1,2,3,5,8,12-A_6B_7	−610.09	−685.05	−797.63				
1,2,3,5,9,10-A_6B_7	−610.50	−684.11	−797.57				
1,2,3,5,9,12-A_6B_7	−610.20	−684.76	−797.54				
1,2,3,5,10,12-A_6B_7	−610.20	−684.76	−797.54				
1,2,3,9,10,12-A_6B_7	−610.31	−684.27	−797.49				
1,2,4,7,8,10-A_6B_7	−611.67	−686.05*	−797.73*				
1,2,4,7,9,10-A_6B_7	−611.79*	−685.75	−797.63				
1,2,4,7,9,12-A_6B_7	−610.19	−684.98	−797.53				
1,2,4,7,10,12-A_6B_7	−611.79*	−685.75	−797.63				
1,2,4,9,11,12-A_6B_7	−610.31	−684.69	−797.40				
1,2,3,4,5,13-B_6A_7	−594.19	−684.03	−821.35*	1,2,3,4,5,6-B_6A_7	−584.54	−748.07	−857.77
1,2,3,4,9,13-B_6A_7	−596.00	−684.29	−821.25	1,2,3,4,5,7-B_6A_7	−586.34	−748.99	−857.82
1,2,3,4,10,13-B_6A_7	−597.70	−684.99	−821.23	1,2,3,4,5,8-B_6A_7	−586.23	−749.15	−857.87
1,2,3,5,8,13-B_6A_7	−597.59	−685.07	−821.32	1,2,3,4,5,9-B_6A_7	−586.34	−748.99	−857.82
1,2,3,5,9,13-B_6A_7	−597.70	−684.80	−821.22	1,2,3,4,5,10-B_6A_7	−588.03	−750.10	−857.92
1,2,3,5,10,13-B_6A_7	−597.70	−684.80	−821.22	1,2,3,4,5,11-B_6A_7	−588.03	−750.10	−857.92
1,2,3,5,12,13-B_6A_7	−599.40	−685.48	−821.23	1,2,3,4,5,12-B_6A_7	−589.72	−751.39	−858.02
1,2,3,9,10,13-B_6A_7	−599.51	−685.30	−821.10	1,2,3,4,9,10-B_6A_7	−589.83	−751.03	−857.97
1,2,4,7,8,13-B_6A_7	−597.60	−685.02	−821.31	1,2,3,4,9,11-B_6A_7	−589.83	−751.05	−857.99
1,2,4,7,9,13-B_6A_7	−599.40	−685.42	−821.22	1,2,3,4,9,12-B_6A_7	−589.83	−751.03	−857.47
1,2,4,7,10,13-B_6A_7	−600.99	−686.50	−821.30	1,2,3,4,10,12-B_6A_7	−591.52	−752.29	−858.05
1,2,4,7,12,13-B_6A_7	−599.40	−685.42	−821.22	1,2,3,5,8,9-B_6A_7	−589.73	−751.02	−858.02
1,2,4,9,11,13-B_6A_7	−599.51	−685.07	−821.14	1,2,3,5,8,10-B_6A_7	−591.41	−752.29	−858.12
1,2,4,10,12,13-B_6A_7	−601.10*	−686.20*	−821.20	1,2,3,5,8,11-B_6A_7	−591.30	−752.45	−858.17
				1,2,3,5,8,12-B_6A_7	−591.41	−752.29	−858.12

Table 3. (continued)

B-centered				A-centered			
formulas	A = Ag B = Au	A = Ni B = Au	A = Pt B = Au	formulas	A = Ag B = Au	A = Ni B = Au	A = Pt B = Au
				1,2,3,5,9,10-B_6A_7	−589.83	−751.01	−857.95
				1,2,3,5,9,12-B_6A_7	−591.52	−752.12	−858.07
				1,2,3,5,10,12-B_6A_7	−591.52	−752.12	−858.07
				1,2,3,9,10,12-B_6A_7	−591.63	−752.10	−857.98
				1,2,4,7,8,10-B_6A_7	−592.99	−753.56*	−858.27*
				1,2,4,7,9,10-B_6A_7	−593.11*	−753.40	−858.22
				1,2,4,7,9,12-B_6A_7	−591.53	−751.96	−858.09
				1,2,4,7,10,12-B_6A_7	−593.11*	−753.40	−858.22
				1,2,4,9,11,12-B_6A_7	−591.64	−751.80	−858.05
1,2,3,4,13-B_5A_8	−583.32	−683.39	−844.70*	1,2,3,4,5-B_5A_8	−573.74	−753.63	−881.90
1,2,3,5,13-B_5A_8	−585.02	−683.65	−844.67	1,2,3,4,9-B_5A_8	−575.54	−754.54	−881.94
1,2,3,9,13-B_5A_8	−586.82	−684.13	−844.54	1,2,3,4,10-B_5A_8	−577.22	−755.78	−882.03
1,2,4,7,13-B_5A_8	−586.72	−684.90	−844.64	1,2,3,5,8-B_5A_8	−577.12	−755.75	−882.08
1,2,4,9,13-B_5A_8	−586.83	−684.21	−844.56	1,2,3,5,9-B_5A_8	−577.23	−755.60	−882.03
1,2,4,10,13-B_5A_8	−588.41	−685.05	−844.62	1,2,3,5,10-B_5A_8	−577.23	−755.60	−882.03
1,2,4,11,13-B_5A_8	−586.83	−684.21	−844.56	1,2,3,5,12-B_5A_8	−578.91	−756.83	−882.13
1,2,4,12,13-B_5A_8	−588.52	−684.60	−844.53	1,2,3,9,10-B_5A_8	−579.02	−756.72	−882.06
1,2,8,9,13-B_5A_8	−588.52	−684.74	−844.51	1,2,4,7,8-B_5A_8	−577.13	−755.62	−882.08
1,2,8,10,13-B_5A_8	−590.11*	−685.76*	−844.60	1,2,4,7,9-B_5A_8	−578.92	−756.67	−882.13
1,2,8,12,13-B_5A_8	−588.52	−684.74	−844.51	1,2,4,7,10-B_5A_8	−580.49	−758.05*	−882.27*
1,2,9,12,13-B_5A_8	−588.63	−684.39	−844.43	1,2,4,7,12-B_5A_8	−578.92	−756.67	−882.13
				1,2,4,9,11-B_5A_8	−579.03	−756.51	−882.09
				1,2,4,10,12-B_5A_8	−580.60*	−757.88	−882.22
1,2,3,13-B_4A_9	−572.25	−680.99	−867.74*	1,2,3,4-B_4A_9	−561.04	−757.27	−905.73
1,2,4,13-B_4A_9	−573.95	−682.01	−867.72	1,2,3,5-B_4A_9	−562.73	−758.30	−905.81
1,2,8,13-B_4A_9	−575.64	−682.41	−867.67	1,2,3,9-B_4A_9	−564.52	−759.34	−905.84
1,2,9,13-B_4A_9	−575.75	−682.46	−867.58	1,2,4,7-B_4A_9	−564.42	−759.35	−905.90
1,7,9,13-B_4A_9	−577.33*	−683.04*	−867.65	1,2,4,9-B_4A_9	−564.53	−759.19	−905.86
				1,2,4,10-B_4A_9	−566.10	−760.53	−905.99
				1,2,4,11-B_4A_9	−564.53	−759.19	−905.86
				1,2,4,12-B_4A_9	−566.21	−760.37	−905.94
				1,2,8,9-B_4A_9	−566.21	−760.37	−905.95
				1,2,8,10-B_4A_9	−567.79*	−761.71*	−906.07*
				1,2,8,12-B_4A_9	−566.21	−760.37	−905.93
				1,2,9,12-B_4A_9	−566.32	−760.21	−905.88
1,2,13-B_3A_{10}	−560.98	−677.42	−890.49*	1,2,3-B_3A_{10}	−548.13	−760.01	−929.35
1,7,13-B_3A_{10}	−562.67	−680.05*	−890.45	1,2,4-B_3A_{10}	−549.82	−761.02	−929.44
1,12,13-B_3A_{10}	−562.78*	−677.55	−890.35	1,2,8-B_3A_{10}	−551.51	−762.18	−929.51
				1,2,9-B_3A_{10}	−551.61	−762.02	−929.46
				1,7,9-B_3A_{10}	−553.19*	−763.32*	−929.59*
1,13-B_2A_{11}	−547.82*	−671.92*	−912.97*	1,2-B_2A_{11}	−535.02	−761.80	−952.76
				1,7-B_2A_{11}	−536.70	−762.93*	−952.83*
				1,12-B_2A_{11}	−536.81*	−762.76	−952.77
13-BA_{12}	−532.76*	−664.19*	−935.19*	1-BA_{12}	−520.01*	−761.62*	−975.86*
				A_{13}	−503.11*	−759.32*	−998.68*

[a] The most stable structures are marked with an asterisk (*).

energy than Ag (see Appendix) and that there are 36 Au−Au bonds and 6 Au−Ag bonds in 1-$AgAu_{12}$ versus 30 Au−Au and 12 Au−Ag bonds in 13-$AgAu_{12}$. Similarly, the Ni-centered 13-$NiAu_{12}$ is more stable than the Au-centered 1-$NiAu_{12}$ by 35.82 kcal/mol (Scheme 2) due to the fact that Ni has a higher cohesive energy than Au (see Appendix). Since the cohesive energy follows the trend Pt > Ni > Au > Ag, we expect the following ranking of the stability of monosubstituted centered icosahedral clusters (see Table 3 for the calculated metallic bonding energies):

$$\text{13-AgAu}_{12}\text{ (Ag-centered)} < \text{1-AgAu}_{12}\text{ (Au-centered)}$$

$$\text{13-AuAg}_{12}\text{ (Au-centered)} > \text{1-AuAg}_{12}\text{ (Ag-centered)}$$

$$\text{13-PtAu}_{12}\text{ (Pt-centered)} > \text{1-PtAu}_{12}\text{ (Au-centered)}$$

$$\text{13-AuPt}_{12}\text{ (Au-centered)} < \text{1-AuPt}_{12}\text{ (Pt-centered)}$$

$$\text{13-NiAu}_{12}\text{ (Ni-centered)} > \text{1-NiAu}_{12}\text{ (Au-centered)}$$

$$\text{13-AuNi}_{12}\text{ (Au-centered)} < \text{1-AuNi}_{12}\text{ (Ni-centered)}$$

In many cases, the Strong-Bond rule implies that metals which are capable of forming strong metal−metal bonds tend to occupy the center position of the icosahedron. Hence, it may also be called the "Central-Atom" rule. In fact, this site preference rule can be applied to any centered icosahedral metal cluster A_nB_{13-n}. As is evident from Table 3, for any given A_nB_{13-n} icosahedral cluster, the center of the icosahedron is always occupied by the "strongest metal" (i.e., the metal with a higher cohesive energy). Further examples can be found in Schemes 3−6. In Scheme 3, the three Au-centered stereoisomers (1,2-, 1,7-, and 1,12-Ag_2Au_{11}) are more stable than the Ag-centered structure (1,13-Ag_2Au_{11}) by ca. 3−5 kcal/mol because gold is a "stronger" metal than silver. In contrast, in Scheme 4, the Ni-centered stereoisomer 1,13-Ni_2Au_{11} is substantially more stable than the three Au-centered stereoisomers by ca. 40−41 kcal/mol since nickel is a "stronger" metal than gold. Similar conclusions can be drawn from Scheme 5: the five Au-centered Ag_3Au_{10} clusters are more stable than the three Ag-centered Ag_3Au_{10} clusters, whereas the reverse is true for the Ni_3Au_{10} clusters (Scheme 6).

It should be pointed out that the center position of a centered icosahedron differs from the surface sites in two important

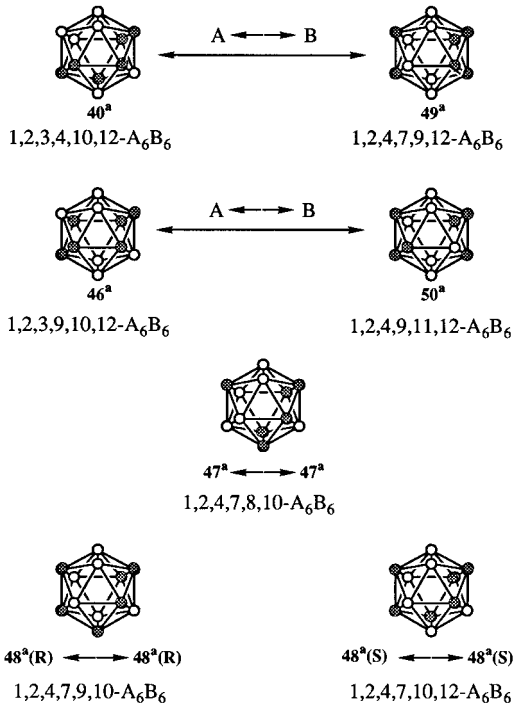

Figure 3. Two examples (top) of "atom inversions" and three examples (bottom) of "self-inversions" of several A_6B_6 stereoisomers (see text).

Scheme 1. Relative Stabilities of $AgAu_{12}$ Stereoisomers (Energy Differences in Parentheses)

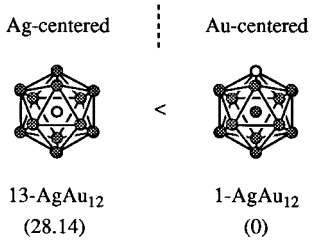

Scheme 2. Relative Stabilities of $NiAu_{12}$ Stereoisomers (Energy Differences in Parentheses)

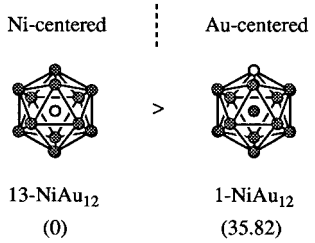

aspects. First, the central atom has 12 center−surface bonds, whereas each surface atom has only six bonds (five surface−surface bonds and one center−surface bond). In fact, this is the *origin* of the Central-Atom rule, which places the atom with the highest cohesive energies in the center of the centered icosahedron for maximum bond (stabilization) energies. Second, a center−surface bond is not equivalent to a surface−surface bond. Indeed, the center−surface (*b*) bonds are somewhat shorter than the surface−surface (*a*) bonds. For an ideal icosahedron, the bond-length ratio (*b*/*a*) is 0.951. For example, the calculated (energy-minimized) center−surface and surface−surface distances in Au_{13} are 2.78 and 2.92 Å, respectively, with a *b*/*a* ratio of 0.951, as expected. This 5% difference in bond lengths implies a 6% disparity in bond energies ($U_b/U_a = 0.937/0.995 = 0.94$) based on the Lennard-Jones potentials (eq 5) utilized. However, since this second effect is present in all centered icosahedral clusters, the relative ordering of the stabilities of the clusters will not be adversely affected. In sum, the numerical advantage (12 vs 6 bonds) of the central atom to form stronger bonds (the first attribute) outweighs the slight difference in the bond energies between the center−surface and surface−surface bonds (the second effect), thereby ensuring the validity of the Central-Atom rule.

Scheme 3. Relative Stabilities of Ag_2Au_{11} Stereoisomers (Energy Differences in Parentheses)

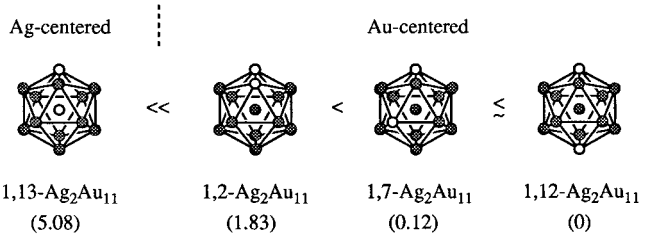

Scheme 4. Relative Stabilities of Ni_2Au_{11} Stereoisomers (Energy Differences in Parentheses)

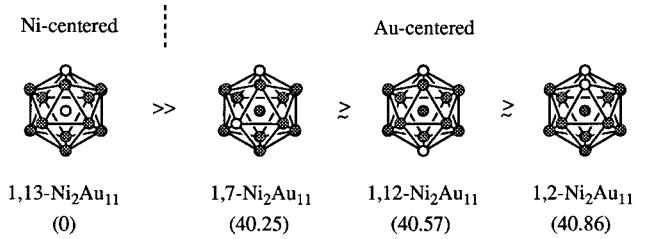

(2) Hetero-Bond Rule: The Ionic Contribution. The second important contribution to the metallic interaction energy is the partial "*ionic* character" of the metal−metal bonds due to the differences in electronegativities of the constituents. This effect gives rise to an extra stabilization energy in addition to the covalent contribution. As a result, the system tends to *maximize* the number of heteronuclear bonds (at the expense of the homonuclear bonds). We shall call this the "Hetero-Bond" rule. It is clear that *ionicity* is the *origin* of the Hetero-Bond rule. It can be seen from Table 3 that the most stable stereoisomers are those with the highest numbers of hetero (A−B) bonds on the surface. In fact, in many cases, this rule governs the arrangement of the surface atoms (surface ordering) of a cluster. Hence, it may also be called "*Surface−Atom*" rule.

A corollary of the Hetero-Bond rule is the "*Non-Nearest-Neighbor*" rule for like atoms. That is, to maximize the number of heteronuclear bonds, like atoms, or more specifically, the minority atoms on the surface of the cluster tend *not* to be neighbors. For example, as depicted in Scheme 3, of the three stereoisomers of the Au-centered Ag_2Au_{11} clusters, the ones in which the two silver atoms are not neighbors (1,7- and 1,12-Ag_2Au_{11}) are more stable than the one (1,2-Ag_2Au_{11}) in which the two silver atoms are bonded to each other (as neighbors) by ca. 1.8 kcal/mol.[28] Without the "ionic character" stabilization of the Au−Ag bonds, these three stereoisomers would have the same energy of −628.88 kcal/mol (see Table 3).

A more useful expression of the Hetero-Bond Rule is the "*Maximum-Fragment*" rule which states that stereoisomers with a higher number of fragments of the minority atoms tend to be

(28) Note also that the 1,12-Ag_2Au_{11} is also slightly (~0.11 kcal/mol) more stable than the 1,7-Ag_2Au_{11} structure, due to the long-range effect (i.e., two to three bond effects) of the Lennard-Jones potential.

Scheme 5. Relative Stabilities of Ag_3Au_{10} Stereoisomers (Energy Differences in Parentheses)

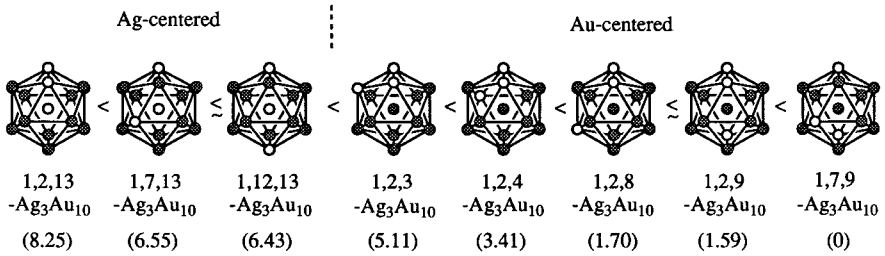

Scheme 6. Relative Stabilities of Ni_3Au_{11} Stereoisomers (Energy Differences in Parentheses)

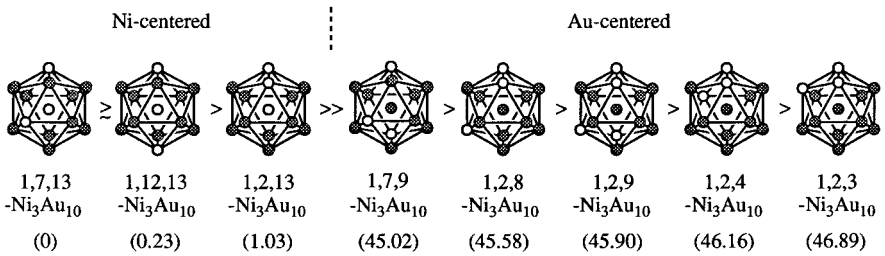

more stable. In other words, in order to maximize the heteronuclear bonds, the minority atoms tend to be "fragmented" (i.e., scattered) on the surface of a cluster. This is borne out by our calculations. As is evident from Tables 2 and 3, stereoisomers with the maximum numbers of fragments (3 > 2 > 1) tend to be more stable.

The three Au-centered Ag_2Au_{11} stereoisomers in Scheme 3 illustrate this point well: the two-fragment stereoisomers 1,7-Ag_2Au_{11} and 1,12-Ag_2Au_{11} are more stable than the one-fragment stereoisomer 1,2-Ag_2Au_{11}. It is also true for the five Au-centered Ag_3Au_{10} stereoisomers in Scheme 5: the one with three minority fragments (1,7,9-Ag_3Au_{10}) is ca. 1.6 kcal/mol more stable than the two-fragment stereoisomers (1,2,8- and 1,2,9-Ag_3Au_{10}) which are in turn ca. 2−3.5 kcal/mol more stable than the one-fragment stereoisomers (1,2,3- and 1,2,4-Ag_3Au_{10}). The same principle applies to the three Ag-centered stereoisomers in Scheme 5 as well as the corresponding Ni_2Au_{11} (Scheme 4) and Ni_3Au_{10} (Scheme 6) series.

The number of stereoisomers increases rapidly with increasing number of minority atoms. Nevertheless, the same principle applies. For example, a graphical representation of the relative metallic energies of Au-centered icosahedral clusters depicted in Figure 4 reveals that the most stable structures are those with the most minority fragments and that the most stable structure 1,2,8,10-Ag_4Au_9 (No. 10 in Figure 4) has the maximum (three) number of minority (Ag) fragments. A similar plot in Figure 5 for the Au-centered icosahedral Ag_6Au_7 clusters gives rise to the same conclusion.

(D) Most Stable Stereoisomers. The most stable structures, on the basis of our calculations, are indicated by asterisks (*) in Table 3. In particular, the most stable stereoisomers of the three icosahedral series A_nB_{13-n} (where $n = 0-12$) are depicted graphically in Figure 6: the Au-centered Ag_nAu_{13-n} (squares), the Ni-centered Au_nNi_{13-n} (triangles), and the Pt-centered Au_nPt_{13-n} (circles). (Note that the corresponding Ag-centered Ag_nAu_{13-n}, the Au-centered Au_nNi_{13-n}, and the Au-centered Au_nPt_{13-n} series (not shown), respectively, are of higher energies, in accordance with the Central-Atom rule.) Within each series, successive replacement of the "strong" metal by a "weaker" metal causes the metallic energy to rise monotonically except in the case of the Ni-centered Au_nNi_{13-n} series where the stepwise replacement of the first six surface Ni atoms by

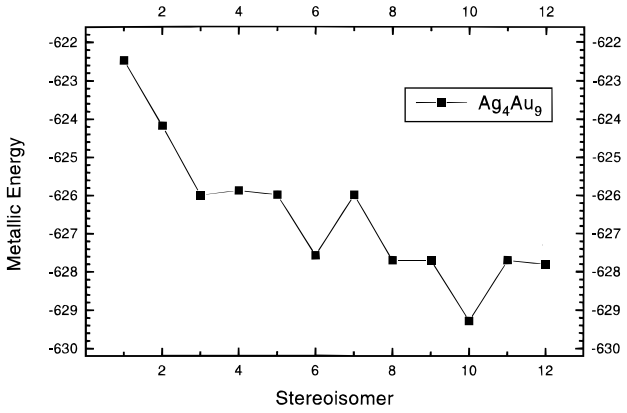

Figure 4. Total metallic energies of the various stereoisomers of Au-centered icosahedral Ag_4Au_9 clusters (from left to right): (1) 1,2,3,4-Ag_4Au_9; (2) 1,2,3,5-Ag_4Au_9; (3) 1,2,3,9-Ag_4Au_9; (4) 1,2,4,7-Ag_4Au_9; (5) 1,2,4,9-Ag_4Au_9; (6) 1,2,4,10-Ag_4Au_9; (7) 1,2,4,11-Ag_4Au_9; (8) 1,2,4,12-Ag_4Au_9; (9) 1,2,8,9-Ag_4Au_9; (10) 1,2,8,10-Ag_4Au_9; (11) 1,2,8,12-Ag_4Au_9; (12) 1,2,9,12-Ag_4Au_9.

Au atoms causes little changes in the total metallic energies. This somewhat anomalous trend may be understood in terms of the small difference in the cohesive energies and a somewhat larger difference in the electronegativities between Au and Ni (cf. Appendix) which translate into a small change in covalent contribution and a large change in the ionic contribution, respectively, to the total metallic energy per substitution. Such a combination gives rise to a smaller slope as is the case for the Au_nNi_{13-n} clusters as n increases (Figure 6).

A detailed examination of the most stable structures in Table 3 confirms the validity of the site preference rules. For example, as portrayed in Figure 7, the most stable stereoisomers of icosahedral Ag_nAu_{13-n} clusters are always Au-centered (Strong-Bond or Center-Atom rule). Of the Au-centered stereoisomers, those with the highest possible numbers of fragments of the minority atoms are the most stable structures (Hetero-Bond or Maximum-Fragment rule). For example, the most stable stereoisomer of Ag_4Au_9 is 1,2,8,10-Ag_4Au_9 which has been observed in $[Ag_4Au_9(PPh_2Me)_8X_4]^+$ where X = Cl,[9c] Br.[9d] Further examination of Figure 7 reveals that the most stable structures of Ag-rich icosahedral clusters mirror those of the Au-rich analogues. One example is the pair of Au-rich 1,2,4,-

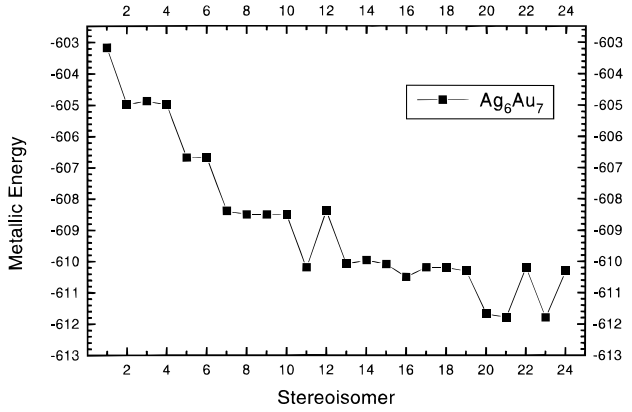

Figure 5. Total metallic energies of the various stereoisomers of Au-centered icosahedral Ag_6Au_7 clusters (from left to right): (1) 1,2,3,4,5,6-Ag_6Au_7; (2) 1,2,3,4,5,7-Ag_6Au_7; (3) 1,2,3,4,5,8-Ag_6Au_7; (4) 1,2,3,4,5,9-Ag_6Au_7; (5) 1,2,3,4,5,10-Ag_6Au_7; (6) 1,2,3,4,5,11-Ag_6Au_7; (7) 1,2,3,4,5,12-Ag_6Au_7; (8) 1,2,3,4,9,10-Ag_6Au_7; (9) 1,2,3,4,9,11-Ag_6Au_7; (10) 1,2,3,4,9,12-Ag_6Au_7; (11) 1,2,3,4,10,12-Ag_6Au_7; (12) 1,2,3,5,8,9-Ag_6Au_7; (13) 1,2,3,5,8,10-Ag_6Au_7; (14) 1,2,3,5,8,11-Ag_6Au_7; (15) 1,2,3,5,8,12-Ag_6Au_7; (16) 1,2,3,5,9,10-Ag_6Au_7; (17) 1,2,3,5,9,12-Ag_6Au_7; (18) 1,2,3,5,10,12-Ag_6Au_7; (19) 1,2,3,9,10,12-Ag_6Au_7; (20) 1,2,4,7,8,10-Ag_6Au_7; (21) 1,2,4,7,9,10-Ag_6Au_7; (22) 1,2,4,7,9,12-Ag_6Au_7; (23) 1,2,4,7,10,12-Ag_6Au_7; (24) 1,2,4,9,11,12-Ag_6Au_7.

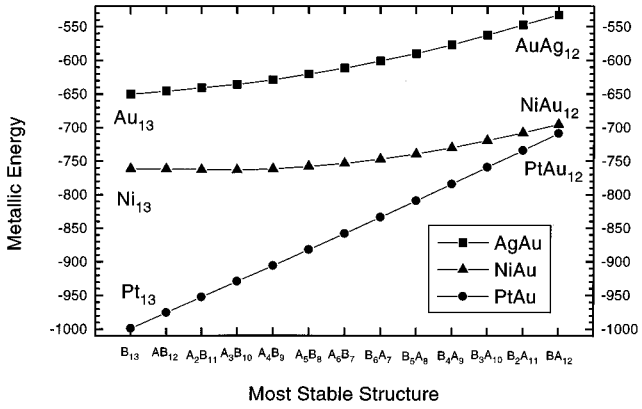

Figure 6. Total metallic energies of the most stable structures of Au-centered icosahedral Ag_nAu_{13-n} (squares), Ni-centered icosahedral Au_nNi_{13-n} (triangles), and Pt-centered icosahedral Au_nPt_{13-n} (circles) clusters. Note that the total metallic energies of the most stable structures of the Ag-centered Ag_nAu_{13-n}, Au-centered Au_nNi_{13-n}, and Au-centered Au_nPt_{13-n} cluster series (not shown) are of higher energies than those of the three series shown here.

10,12-Ag_5Au_8($32_B{}^a$) and the Ag-rich 1,2,4,10,12,13-Au_6Ag_7-($32_B{}^b$). Both are Au-centered and both have the same arrangement of the minority atoms (Ag in $32_B{}^a$ and Au in $32_B{}^b$). Here a and A stand for Ag and b and B for Au.

One of the motivations of the present work is to predict the energetically most favored Ag_6Au_7 stereoisomers as building blocks of the vertex-sharing polyicosahedral Au−Ag cluster series synthesized and structurally characterized by us.[11] Our calculations show that the most stable structures of the Ag_6Au_7 icosahedral clusters are the chiral pair 1,2,4,7,9,10-Ag_6Au_7 ($48_B{}^a$(R)) and 1,2,4,7,10,12-Ag_6Au_7 ($48_B{}^a$(S)) of C_1 symmetry as portrayed in Figure 7 (bottom). The arrangement of the minority (A) atoms on the surface of these two structures resembles the shape of a "hook". These structures are presently unknown. However, the next most stable stereoisomer (only 0.12 kcal/mol higher in energy) 1,2,4,7,8,10-Ag_6Au_7 ($47_B{}^a$), of C_{5v} symmetry, which resembles the shape of a "top", also depicted in Figure 7, has been observed as the building blocks in an extensive series of vertex-sharing biicosahedral clusters[11]

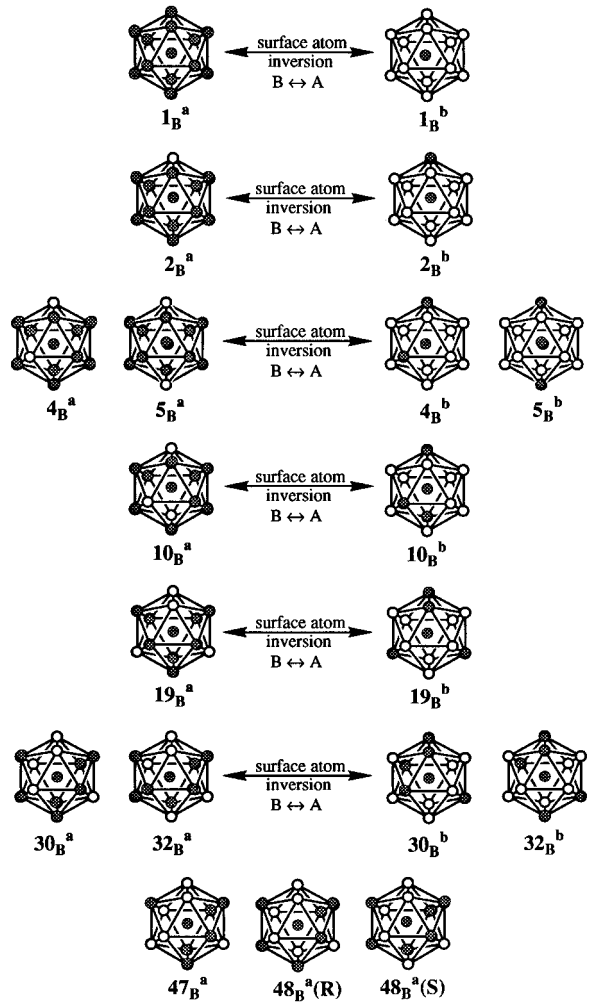

Figure 7. Most stable stereoisomers of Au-centered Ag_nAu_{13-n} clusters. Here Ag and Au are represented by open and shaded circles and designated as A and B, respectively. The double arrows indicate surface inversions only.

as exemplified by $[(Ph_3P)_{10}Au_{13}Ag_{12}Br_8]^+$ (see Figure 8b for the metal framework). Furthermore, the "Ag_6-boat"-structure of 1,2,4,7,9,12-Ag_6Au_7 ($49_B{}^a$), of C_{2v} symmetry, is the building block for vertex-sharing triicosahedral Au−Ag clusters (Figure 8c) as exemplified by $[(Ph_3P)_{12}Au_{18}Ag_{20}Cl_{14}]$.[11] Likewise, the "$Ag_6$-chair" structure of 1,2,4,9,11,12-Ag_6Au_7 ($50_B{}^a$) is the building block for the vertex-sharing tetraicosahedral cluster $[L_{12}Au_{22}Ag_{24}X_{14}]$ (Figure 8d).[11] An examination of the calculated energies in Table 3 showed that these building blocks for vertex-sharing polyicosahedral clusters are among the next most stable stereoisomers (within 1.5 kcal/mol). The utilization of the most stable stereoisomers of a single icosahedron as the building blocks for vertex-sharing polyicosahedral clusters s_n ($n = 1-4$) portrayed in Figure 8 signifies the energetic control in the "progressive growth" of this particular cluster sequence. Furthermore, the fact that the basic building blocks of the vertex-sharing polyicosahedral clusters are among the most stable stereoisomers lends further credence to the "cluster of clusters" concept.[11] In other words, we believe that the formation of the 13-atom centered icosahedron (building block) precedes the polyicosahedral growth via vertex-sharing. Of course the observed structures represent a compromise of bonding (both metal−metal and metal−ligand interactions), symmetry, and packing of the ligands. In this regard, we predict that the highly symmetrical D_{3d} structure of 1,2,3,9,10,12-Ag_6Au_7 ($46_B{}^a$)

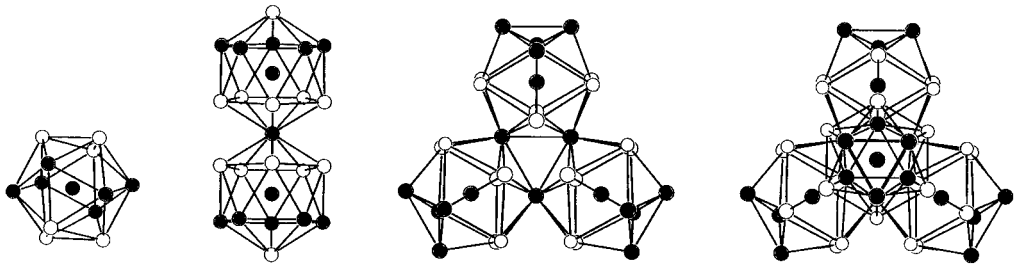

$s_1(13)$	$s_2(25)$	$s_3(36)$	$s_4(46)$
"Au_6 chair"	"top"	"Ag_6 boat"	"Ag_6 chair"
1,2,3,9,10,12-Ag_6Au_7	1,2,4,7,8,10-Ag_6Au_7	1,2,4,7,9,12-Ag_6Au_7	1,2,4,9,11,12-Ag_6Au_7
$46_B{}^a$	**$47_B{}^a$**	**$49_B{}^a$**	**$50_B{}^a$**
(1.48)	(0.12)	(1.60)	(1.48)
(a)	**(b)**	**(c)**	**(d)**

Figure 8. Progressive growth of the early members of vertex-sharing polyicosahedral Au−Ag cluster series, $s_n(N)$, where $n = 1-4$ and N is the nuclearity. The second to fourth rows give, respectively, the descriptions, the nomenclatures, and the designators of the icosahedral building blocks. The numbers in parentheses (the fifth row) indicate the energy differences between each of these building blocks and the most stable structures $48_B{}^a$(R) and $48_B{}^a$(S) (see Table 3). (Au in shaded circles and Ag in open circles).

portrayed in Figure 8a will be a good candidate for the as yet unknown structure of a monoicosahedral Ag_6Au_7 cluster.

V. Conclusion

"Site preference" is a manifestation of the disparity in the bonding capabilities of the different metal constituents in heterometallic clusters.[19] If we ignore effects such as ligand bonding and charge distribution, there are two major components to the metal−metal bonding in a metal cluster: the covalent and the ionic contributions. These two components were modeled by use of the cohesive energies and Pauling's electronegativities, respectively, in this paper. The distance dependence of the metallic bonding energy was modeled by the Lennard-Jones potential. The total metallic bond energy, U_m, is defined as the sum of all pairwise metal−metal bonding interactions. And finally, the structure of each stereoisomer was optimized by minimizing U_m with respect to all distances.

On the basis of the calculated bond energies tabulated in Table 3, two site preference rules—the Strong-Bond rule and the Hetero-Bond rule—can be formulated. These rules are extremely useful in ascertaining the relative stabilities of the stereoisomers of various icosahedral mixed-metal clusters. The Strong-Bond rule, which stems from the covalent contribution, states that stereoisomers having a higher number of "strong bonds" tend to be more stable. In many cases, the Strong-Bond rule implies that metals which are capable of forming strong metal−metal bonds tend to occupy the center position of the icosahedron. Hence, it may also be called the "Central-Atom" rule. The Hetero-Bond rule, which originates from the "*ionic* character" of heterometallic bonds, tends to *maximize* the number of heteronuclear bonds. In many cases, this rule governs the arrangement of the surface atoms (surface ordering) of a cluster. Hence, it may also be called "Surface-Atom" rule. A corollary to the Hetero-Bond rule is the "Non-Nearest-Neighbor" rule for like atoms. That is, in order to maximize the number of heteronuclear bonds, like atoms, or more specifically, the minority atoms on the surface of the cluster tend not to be neighbors. Yet another manifestation of the Hetero-Bond rule is the "Maximum-Fragment" rule, which states that stereoisomers with a higher number of fragments of the minority atoms tend to be more stable (see below).

An examination of the most stable structures in Table 3 confirms the validity of the site preference rule established here (see Schemes 1−6). For example, for Ag_nAu_{13-n} icosahedral clusters, the most stable stereoisomers are always Au-centered (Strong-Bond or Center-Atom rule). Furthermore, of the Au-centered stereoisomers, those with the highest possible numbers of fragments of the minority atoms are the most stable structures (Hetero-Bond or Maximum-Fragment rule). The same site preference principles apply to Ni_nAu_{13-n} (as well as Pt_nAu_{13-n}) icosahedral clusters. Here the most stable stereoisomers are all Ni- or Pt-centered (Strong-Bond rule), and the minority atoms on the surface follow the Maximum-Fragment rule (Hetero-Bond rule).

The methodology for determining the relative stabilities of mixed-metal clusters described in this paper differs from other widely used approaches, such as the tight-binding model,[29,30] the embedded-atom method (EAM),[31] the effective medium theory (EMT),[32] and density function theory.[33] Basically, the present approach is a static (thermodynamic) model which takes into account all pairwise interactions (i.e., not just the nearest neighbors as in the tight-binding model or the host medium approach as in EAM or EMT), as modeled by the Lennard-Jones potential. A novel feature of our method is that it explicitly takes into account the ionic character of heterometallic bonds. The minimized total metallic bond energies for the various stereoisomers represent the relative ordering of the energetics of the ground-state configurations. Furthermore, the results presented in this paper are in excellent agreement with those based on other more elaborate calculations. For example, the most stable stereoisomers of icosahedral Ag_nAu_{13-n} clusters based on our static calculations (Figure 7 in this paper) are fully consistent with the ground-state atomic configurations of icosahedral Al_nNi_{13-n} clusters calculated by Rey, Garcia-Rodeja, and Gallego[31a] via molecular-dynamic simulations using the embedded-atom method (Figure 4 in ref 31a).

(29) Ducastelle, F. *J. Phys. (Paris)* **1970**, *31*, 1055.
(30) Massobrio, C.; Pontikis, V.; Martin, G. *Phys. Rev. B* **1990**, *41*, 10486.
(31) (a) Rey, C.; Garcia-Rodeja, J.; Gallego, L. J. *Phys. Rev. B* **1996**, *54*, 2942. (b) Montejano-Carrizales, J. M.; Iniguez, M. P.; Alonso, J. A.; Lopez, M. J. *Phys. Rev. B* **1996**, *54*, 5961. (c) Katagiri, M.; Kubo, M.; Yamauchi, R.; Miyamoto, A.; Nozue, Y.; Terasaki, O.; Coley, T. R.; Li, Y. S.; Newsam, J. M. *Jpn. J. Appl. Phys.* **1995**, *34*, 6866. (d) Foiles, S. M.; Baskes, M. I.; Daw, M. S. *Phys. Rev. B* **1986**, *33*, 7983.
(32) Stott, M. J.; Zaremba, E. *Phys. Rev. B* **1980**, *22*, 1564.
(33) (a) Hohenberg, P.; Kohn, W. *Phys. Rev.* **1964**, *136*, B864. (b) Alonso, J. A. *Phys. Scr.* **1994**, *55*, 177.

It is remarkable that the simple approach to metallic bonding outlined in this paper is capable of predicting the relative stabilities of structures of stereoisomers of mixed-metal icosahedral clusters. The same methodology can be applied to other cluster systems and metal combinations. In fact, since the cohesive energies and the equilibrium interatomic distances of all three series of transition metals are known, calculations similar to those described in this paper can be applied to other cluster geometries and metal combinations (work in progress).

Finally, it should be reiterated that the site preference rules developed in this paper apply to transition metal clusters or intermetallic systems where metal−metal bonding is dominant. Furthermore, these rules also apply, in general, to intermetallic phases[34] which may contain main-group elements as part of the cluster framework (e.g., the 1,2,8,10-A_4B_8 stereoisomer predicted by the Surface-Atom rule was found in $SrAu_{5+x}Al_{7-x}$). However, in cases where the ligands coordinate strongly and selectively to the metal component with the higher cohesive energy, reversal of the Central-Atom rule may occur (e.g., the vertex-sharing tetraoctahedral cluster $[Au_6Ni_{12}(CO)_{24}]^{2-}$ [35] has a Au-rich, instead of Ni-rich, cluster core because the carbonyl ligands strongly and selectively coordinate to the nickel atoms).[36]

In cases where strong bonding effects between main-group elements are present, deviation from the Surface-Atom rule may occur (e.g., the icosahedral cluster $[Te_4Ni_8(CO)_{12}]^{2-}$ [37] has a surface atom arrangement of 1,2,9,12-Te_4Ni_8, instead of the expected 1,2,8,10-Te_4Ni_8). Work is in progress to address these occurrences, as well as to extend the present work to intermetallic phases and solid state materials, and results will be forthcoming.

Acknowledgment is made to the National Science Foundation and the donors of the Petroleum Research Fund, administrated by American Chemical Society, for the financial support of this research. We thank Professor L. F. Dahl of University of Wisconsin (Madison) for helpful discussions and H. Dang, Y. Kean, and P. Wang for their assistance in the early stage of this work in terms of model building and preliminary calculations.

Appendix

The table included here (Table 4) lists the parameters used in the calculations.

Table 4. Parameters Used in the Calculations

	ϵ^a (kcal/mol)	χ^b	d^c (Å)
Cu	13.45	1.90	2.556
Ag	11.35	1.93	2.889
Au	14.67	2.54	2.886
Ni	17.13	1.91	2.492
Pd	15.00	2.20	2.751
Pt	22.53	2.28	2.775

[a] Covalent contribution to the metallic bond energy (per bond) $\epsilon = \Delta H^0_{298}/6$, where ΔH^0_{298} is the heat of atomization of bulk metal. [b] Pauling's electronegativity. [c] Nearest-neighbor distances in bulk metal.

IC980006D

(34) For a review on the bonding patterns in intermetallic phases, see: Nesper, R. *Angew. Chem., Int. Ed. Engl.* **1991**, *30*, 789.

(35) (a) Woolery, A. J.; Dahl, L. F. *J. Am. Chem. Soc.* **1991**, *113*, 6684. (b) Johnson, A. J. W.; Spencer, B.; Dahl, L. F. *Inorg. Chim. Acta* **1994**, *227*, 269.

(36) Similar reversals of surface/core metal compositions are also experimentally documented from surface-science studies of bimetallic systems (denoted as the chemisorption-induced aggregation model) if an adsorbate gas binds much more strongly to the metal component with the higher cohesive energy (e.g., Pt−Au alloys in ultrahigh vacuum vs in the presence of CO). See, for example: (a) Sinfelt, J. H. *Acc. Chem. Res.* **1987**, *20*, 134. (b) Sachtler, W. M. H.; van Santen, R. A. *Adv. Catal.* **1997**, *26*, 69. (c) Sinfelt, J. H. *Prog. Solid State Chem.* **1975**, *10*, 55.

(37) Kahaian, A. J.; Thoden, J. B.; Dahl, L. F. *J. Chem. Soc., Chem. Commun.* **1992**, 353.